

1 **Research article**

2 **Full title: GluD1 knockout mice with a pure C57BL/6N background**
3 **show impaired fear memory, social interaction, and enhanced**
4 **depressive-like behavior**

5

6 **Short title: Behavioral and biochemical analyses of GluD1 knockout**
7 **mice with a pure C57BL/6N background**

8

9 Chihiro Nakamoto^{1,2,3}, Meiko Kawamura¹, Ena Nakatsukasa¹, Rie Natsume¹, Keizo
10 Takao^{4,5}, Masahiko Watanabe⁶, Manabu Abe^{1*}, Tomonori Takeuchi^{2,3*}, Kenji Sakimura¹

11

12 **1** Department of Animal Model Development, Brain Research Institute, Niigata

13 University, Niigata, Japan

14 **2** Department of Biomedicine, Aarhus University, Aarhus, Denmark

15 **3** Danish Research Institute of Translational Neuroscience – DANDRITE, Nordic-EMBL

16 Partnership for Molecular Medicine, Aarhus University, Aarhus, Denmark

17 **4** Graduate School of Innovative Life Science, University of Toyama, Toyama, Japan

18 **5** Life Science Research Center, University of Toyama, Toyama, Japan

19 **6** Department of Anatomy, Faculty of Medicine, Hokkaido University, Sapporo, Japan

20

21 * Corresponding authors: tomonori.takeuchi@biomed.au.dk (T. Takeuchi) and

22 manabu@bri.niigata-u.ac.jp (M. Abe).

23 **Abstract**

24 The GluD1 gene is associated with susceptibility for schizophrenia, autism, depression,
25 and bipolar disorder. However, the function of GluD1 and how it is involved in these
26 conditions remain elusive. In this study, we generated a GluD1-knockout (GluD1-KO)
27 mouse line with a pure C57BL/6N genetic background and performed several
28 behavioral analyses. Compared to a control group, GluD1-KO mice showed no
29 significant anxiety-related behavioral differences, evaluated using behavior in an open
30 field, elevated plus maze, a light-dark transition test, the resident-intruder test of
31 aggression and sensorimotor gating evaluated by the prepulse inhibition test. However,
32 GluD1-KO mice showed (1) hyper locomotor activity in the open field, (2) decreased
33 sociability and social novelty preference in the three-chambered social interaction test,
34 (3) impaired memory in contextual, but not cued fear conditioning tests, and (4)
35 enhanced depressive-like behavior in a forced swim test. Pharmacological studies
36 revealed that enhanced depressive-like behavior in GluD1-KO mice was restored by the
37 serotonin reuptake inhibitors imipramine and fluoxetine, but not the norepinephrine
38 transporter inhibitor desipramine. In addition, biochemical analysis revealed no
39 significant difference in protein expression levels, such as other glutamate receptors in
40 the synaptosome and postsynaptic densities prepared from the frontal cortex and the
41 hippocampus. These results suggest that GluD1 plays critical roles in fear memory,
42 sociability, and depressive-like behavior.

43

44

45

46 **Introduction**

47 The δ -type ionotropic glutamate receptor consists of GluD1 (GluR δ 1) and GluD2
48 (GluR δ 2) [1–3]. Despite having conserved membrane topology and amino acid residues
49 critical for glutamate binding and Ca²⁺ permeability, the δ subfamily members do not
50 function as conventional glutamate-gated receptor channels when expressed alone or in
51 combinations with other ionotropic glutamate receptor subunits [4–6]. Instead, they are
52 components of a tripartite transsynaptic adhesion system, where the extracellular domain
53 of postsynaptic GluD1/2 interacts with that of presynaptic neurexin protein (NRXN) via
54 members of the cerebellin precursor protein (CBLN) family in the synaptic cleft [7–9].
55 Moreover, slow activity of GluD1/2 ion channels is triggered by activation of group 1
56 metabotropic glutamate receptors (mGluRs) [10–12].

57 GluD2 has been intensively studied since it was cloned in 1993 [2,3]. In the rodent
58 cerebellum, GluD2 is exclusively expressed in Purkinje cells and is selectively localized
59 to postsynaptic spines at parallel fiber synapses [13,14]. GluD2 is indispensable during
60 the formation and maintenance of parallel fiber-Purkinje cell synapses by interaction with
61 presynaptic neurexins through its amino-terminal domain [7,8,15,16]. In addition, GluD2
62 regulates cerebellar synaptic plasticity [15,17] and motor learning [15,18,19] by
63 interaction with the scaffolding proteins through its carboxyl-terminal domain [20–22].

64 The gene encoding GluD1 in humans (*GRID1*) is associated with a susceptibility
65 for schizophrenia [23–26], major depressive disorder [27], and autism spectrum disorder
66 [28–31]. GluD1 is expressed in various brain regions in rodents, including the cerebral
67 cortex, hippocampus, amygdala, bed nucleus of the stria terminalis, striatum, thalamus,
68 nucleus accumbens, lateral habenular, and the dorsal raphe nucleus [3,32,33]. Similar to

69 GluD2, postsynaptic GluD1 is required for synapse formation and maintenance *in vitro*
70 via CBLN1/CBLN2 and presynaptic NRXN [7,9,34,35]. In addition, GluD1 regulates
71 group 1 mGluRs-mediated long-term depression in the hippocampus *ex vivo* [36].
72 Furthermore, activation of group 1 mGluRs trigger the opening of GluD1 channels,
73 which are key determinants of the slow excitatory postsynaptic current *ex vivo* [12].

74 The GluD1 knockout (GluD1-KO) mice line (*Grid1*^{tm1Jnz}), compared to the
75 relevant control groups, showed abnormal behavioral phenotypes, such as hyper
76 locomotor activity, lower anxiety-like behavior, hyper aggression, higher depression-like
77 behavior, deficits in social interaction [37], enhanced working memory, deficit in
78 contextual and cued fear conditioning [38], and increased stereotyped behavior [39].
79 However, the *Grid1*^{tm1Jnz} mouse was generated from embryonic stem (ES) cells
80 derived from the 129/SvEv strain, followed by backcrossing to C57BL/6 mice 2–6
81 times [37,38,40]. It is well known that backcrossing with different mouse strains leads
82 to a change in the basal levels of behaviors, such as anxiety [41–43], aggression [44,45],
83 prepulse inhibition [46], social interaction [47,48], pain sensitivity [49], depressive-like
84 behavior [42,50–52], and learning and memory [41,53–56]. Thus, a concern of using a
85 mixed genetic background is that the resulting phenotype cannot be confidently
86 attributed to either the target gene or closely-linked genes flanking the targeted locus
87 [53,57,58]. In addition, the 129S6/SvEvTac strain used in *Grid1*^{tm1Jnz} lacked the
88 DISC1 gene (disrupted in schizophrenia 1) [59–61], which is a strong candidate gene
89 that contributes to cause schizophrenia and autism spectrum disorder [62,63]. Moreover,
90 the *Grid1*^{tm1Jnz} mouse was generated by knock-in of a selection marker of neomycin

91 cassette; the promoter of the cassette unexpectedly affected gene expression levels
92 [64–67].

93 To avoid these issues, we generated GluD1-KO mice with a pure C57BL/6N
94 genetic background and investigated an impact of GluD1 deletion on various behaviors
95 including anxiety, aggression, sensorimotor gating, sociability, learning and memory,
96 and depression.

97

98 **Methods**

99 **Animals**

100 GluD1-KO mice were generated using the C57BL/6N ES cell line, RENKA [65] and
101 maintained in a pure C57BL/6N background [68]. Briefly, exon 4 of the *Grid1* gene and
102 a *Pgk* promoter-driven neomycin-resistance cassette were flanked by loxP sequences
103 (*Grid1*^{fllox}). *Grid1*^{fllox} mice were crossed with telencephalin-Cre mice [69] to create the
104 null allele (*Grid1*[−]). Mice were fed *ad libitum* with standard laboratory chow and water
105 in standard animal cages in a 12-h light/dark cycle (light on at 8:00 a.m.) at room
106 temperature and relative humidity in the ranges of 22°C–24°C and 30%–70%,
107 respectively. Experimental protocols used throughout the study were approved by an
108 institutional committee at Niigata University (SA00466) and were in accord with
109 Japanese legislation concerning animal experiments.

110 Behavioral tests were carried out with 8 to 12-week-old male wild-type (WT,
111 *Grid1*^{+/+}) (n = 115 in total) and GluD1-KO (*Grid1*^{−/−}) (n = 92 in total) litter mates by
112 heterozygous breeding, and were performed during the light phase (between 10:00 a.m.

113 and 18:00 p.m.). Mice were handled (3 min per day for 3 days) before starting
114 behavioral tests. Behavioral analyses were performed with the experimenter blind to
115 mice genotype. After each trial, the apparatus was cleaned with hypochlorous water to
116 prevent a bias due to olfactory cues. A battery of behavioral tests were performed in the
117 following order: open field, light-dark transition, elevated plus maze, 3-chamber social
118 interaction, and a forced swim.

119

120 **Open field**

121 Open field tests were carried out using a method similar to that reported previously,
122 with minor modification [70]. Each mouse was placed in the corner of an open field
123 apparatus (50 cm × 50 cm × 40 cm high; O'Hara & Co., Tokyo, Japan) with a chamber
124 illuminated at either 5 or 100 lux. Distance traveled and time spent in the central area
125 (defined as 25% of total area) were recorded and calculated automatically over a 10-min
126 period using Image OFCR software (O'Hara & Co.; see 'Image analysis for behavioral
127 tests').

128

129 **Elevated plus maze**

130 Elevated plus maze tests were carried out using a method similar to that reported
131 previously, with minor modification [70]. The apparatus consisted of two open arms (25
132 cm × 5 cm) and two enclosed arms of the same size with transparent walls (height 15
133 cm). The arms and central square (5 cm × 5 cm) were made of white plastic plates and
134 were elevated 60 cm above the floor (O'Hara & Co.). Arms of the same type were
135 oriented opposite from each other. Each mouse was placed in the central square of the

136 maze, facing one of the closed arms. The time spent in closed and open arms and the
137 frequency of entry into open arms were observed for 10 min under two different
138 illumination condition (5 and 100 lux). Data acquisition was performed automatically
139 using Image EP software (O'Hara & Co.; see 'Image analysis for behavioral tests').

140

141 **Light-dark transition test**

142 Light-dark transition tests were carried out using a method similar to that reported
143 previously, with minor modification [70]. The apparatus consisted of a cage (21 cm ×
144 42 cm × 25 cm high) divided into 2 equal chambers by a black partition containing a
145 small opening (5 cm x 3 cm high) (O'Hara & Co.). One chamber was made of white
146 plastic and was brightly illuminated (252 lux), whereas the other chamber was made of
147 black plastic and was dark (no illumination). Mice were placed in the dark chamber and
148 allowed to move freely between the two chambers for 10 min. Time spent in each
149 chamber, total number of transitions and latency to the first transition from dark to light
150 chambers were recorded automatically using Image LD software (O'Hara & Co.; see
151 'Image analysis for behavioral tests').

152

153 **Resident-intruder test**

154 Resident-intruder tests were carried out using a method similar to that reported
155 previously [37]. Resident male WT (27.3 ± 0.2 g) or GluD1-KO mice (24.1 ± 0.4 g)
156 were individually housed for 3-4 weeks before testing. Resident mice were exposed to
157 intruder male WT C57BL/6 mice, which had been group-housed (four to five per cage)
158 and were of lower body-weight than resident mice (0-4 g lighter than intruder mice), for

159 a duration of 10 min. New intruder mice were used in each test. Latency to attack the
160 intruder and attack frequency were measured manually.

161

162 **Prepulse inhibition test**

163 Acoustic startle response and prepulse inhibition (PPI) of the acoustic startle response
164 were measured using a startle chamber (SR-Lab Systems; San Diego Instruments, CA,
165 USA)[71]. For acoustic startle responses, a background of white noise was used (70 db).
166 An animal was placed in the Plexiglass cylinder and each test session began after 5 min
167 of acclimatization. Mice were presented with 64 trials. There were eight different sound
168 levels presented: 75, 80, 85, 90, 95, 100, 110, and 120 dB. Each white-noise stimulus
169 was 40 ms and presented 8 times in a pseudorandom order such that each sound level
170 was presented within a block of 8 trials. The intertrial interval was 15 s. Analysis for
171 startle amplitudes was based on the mean of the seven trials (ignoring the first trial) for
172 each trial type.

173 PPI responses were measured with acoustic stimuli (120 dB) combined with four
174 different prepulse intensities. Each mouse was placed in the startle chamber and initially
175 acclimatized for 5 min with background white noise alone (70 dB). Mice were then
176 presented with 48 trials. Each session consisted of six trial types. One trial type used a
177 sound burst (40 ms, 120 dB) as the startle stimulus (startle trials). There were four
178 different trials consisting of acoustic prepulse and acoustic startle stimuli (prepulse
179 trials). The prepulse stimulus (20 ms) of either 73, 76, 79, or 82 dB was presented 100
180 ms before the onset of the acoustic startle stimulus. Finally, there were trials where no
181 stimulus was presented (no-stimulus trials). The six trial types were presented in a
182 pseudorandom order such that each trial type was presented once within a block of eight

183 trials. The intertrial interval was 15 s. Analysis was based on the mean of the seven
184 trials (ignoring the first trial) for each trial type. The percentage PPI of a startle response
185 was calculated using the following equation: $100 - [100 \times (\text{startle response on prepulse}$
186 $\text{trials} - \text{no stimulus trials}) / (\text{startle trials} - \text{no stimulus trials})]$.

187

188 **Three-chambered social interaction test**

189 The three-chambered social interaction test was performed as previously described, with
190 minor modification [48,70]. The apparatus consisted of a rectangular, illuminated (5
191 lux) three-chambered box with a lid and an attached infrared video camera (O'Hara &
192 Co.). Each chamber was 20 cm × 40 cm × 22 cm (high) and the dividing walls were
193 made of clear Plexiglas, with small square openings (5 cm wide × 3 cm high) to allow
194 exploration of each chamber. Male mice of the C3H strain, with ages ranging between 8
195 to 12 weeks, were purchased from Charles River Laboratories (Yokohama, Japan) and
196 used as 'strangers'.

197 One day before testing, the 'subject mice' were individually placed in the middle
198 chamber and allowed to freely explore the entire apparatus for 5 min. Before testing,
199 subject mice were placed in the middle chamber and allowed to freely explore all three
200 chambers for 10 min (habituation trial). In the sociability test (sociability trial), an
201 unfamiliar C3H male mouse ('stranger 1') that had no prior contact with the subject
202 mouse was placed in one of the side chambers. The stranger mouse was enclosed in a
203 small, round wire cage, which allowed nose contact between the bars but prevented
204 fighting. This cage was 11 cm in height, with a floor diameter of 9 cm and vertical bars
205 0.5 cm apart. The subject mouse was placed in the middle chamber and presented with
206 stranger 1 in one compartment and an empty cage in another compartment for 10 min.

207 The amount of time spent around each cage (stranger 1 or empty) was measured. At the
208 end of the 10-min sociability trial, each subject mouse was then tested in a 10-min trial
209 to quantitate social preference for a new stranger (social novelty preference trial). The
210 wire cage enclosing the familiar C3H male mouse (stranger 1) was moved to the
211 opposite side of the chamber that had been empty during the sociability trial. A second,
212 unfamiliar C3H male mouse (stranger 2) was placed in the other side of the chamber in
213 an identical small wire cage. The subject mouse was free to explore the mouse from the
214 previous sociability test (stranger 1), and the novel mouse (stranger 2). The amount of
215 time spent around each cage (stranger 1 or stranger 2) was measured. Data acquisition
216 and analysis were performed automatically using Image CSI software (O'Hara & Co.;
217 see 'Image analysis for behavioral tests').

218

219 **Contextual and cued fear conditioning test**

220 The contextual and cued fear conditioning test was performed using a method similar to
221 a previous report [70], with minor modifications. Fear conditioning was conducted in a
222 transparent acrylic chamber (33 cm \times 25 cm \times 28 cm high) with a stainless-steel
223 grid floor (0.2 cm-diameter, spaced 0.5 cm apart; O'Hara & Co.). For the conditioning
224 (conditioning test), each mouse was placed in the chamber and was allowed to explore
225 freely for 3 min. Subsequently, white noise (55 dB) was played through a speaker set on
226 top of the conditioning chamber wall, which served as the conditioning stimulus (CS),
227 was presented for 20 s. During the last 2 s of CS presentation, mice received a
228 footshock (0.7 mA, 2 s), which served as an unconditioned stimulus (US). Two more
229 CS-US pairings were presented with a inter-stimulus interval of 40 s. Animals were
230 returned to their home cages 40 s after the last CS-US paring. Twenty-four hours after

231 conditioning (contextual test), contextual fear memory was tested for 3 min in the same
232 chamber. Forty-eight hours after conditioning (cued test), cued fear memory was tested
233 with an altered context. Each mouse was placed in a triangular chamber (33 cm × 33
234 cm × 32 cm high) made of opaque white plastic and allowed to explore freely for 1
235 min. Subsequently, each mouse was given CS presentation for 3 min. In each session,
236 percentage of time spent freezing was calculated automatically using Image FZ software
237 (O'Hara & Co.; see 'Image analysis for behavioral tests').

238 Pain sensitivity was measured as a control experiment using the fear conditioning
239 chamber apparatus in a manner similar to a previous study [38]. Following 2 min of
240 habituation, mice were given footshocks of increasing strength ranging from 0.05 to 0.7
241 mA in a stepwise manner by 0.05 mA, with an intertrial interval of 30 s. We measured
242 current thresholds for three reactions of mice to nociceptive shock: flinch, vocalization,
243 and jump (vertical and horizontal). Scoring indicated the first shock intensity at which
244 each pain reaction was detected.

245

246 **Forced swim test with pharmacological manipulation**

247 Forced swim tests were performed following Porsolt's method with minor
248 modifications [37,72]. The apparatus consisted of a transparent plastic cylinder (22 cm
249 height; 12 cm diameter) placed in a box (41 cm × 31 cm × 42 cm high; O'Hara & Co).
250 The cylinder was filled with water (22 ± 1°C) up to a height of 10 cm. Each mouse was
251 placed into the cylinder and activity was monitored for 5 min via a CCD camera
252 mounted on the top of the box. The cylinder was refilled with clean water after each test.
253 Image data acquisition and analysis were performed automatically using Image PS
254 software (see 'Image analysis for behavioral tests').

255 With respect to drugs, saline (0.9% NaCl in H₂O) was used as a vehicle and for
256 control injections. Drug concentration for injections were: 15 mg/kg of imipramine
257 (097-06491; FUJIFILM Wako Pure Chemical Corporation, Osaka, Japan), 10 mg/kg of
258 fluoxetine (F132; Sigma-Aldrich, MO, USA), 30 mg/kg of desipramine (042-33931;
259 FUJIFILM Wako Pure Chemical Corporation). Drug concentrations were chosen on the
260 basis of previous studies for imipramine [52][73][74][75][76], fluoxetine
261 [52][73][77][76], and desipramine[52][73][74][76][78]. Both vehicle and drug solutions
262 were intraperitoneally administered. Sixty min after injection, mice were tested in the
263 open field for 10 min with 5 lux illumination and subsequently subjected to a forced swim
264 test for 5 min.

265

266 **Image analysis for behavioral tests**

267 The application software used for the behavioral studies (Image OFCR, LD, EP, CSI,
268 PS, and FZ) were based on the public domain NIH Image program (developed at the
269 U.S. National Institutes of Health and available at <http://rsb.info.nih.gov/nih-image/>)
270 and ImageJ program (<http://rsb.info.nih.gov/ij/>), which were modified for each test
271 (available through O'Hara & Co.).

272

273 **Subcellular fraction and western blot analysis**

274 Subcellular fractions were prepared following Carlin's method [79] with minor
275 modifications. All processes were carried out at 4 °C. Briefly, WT and GluD1-KO mice
276 with a C57BL/6N background (8 to 12 weeks old) were decapitated after cervical
277 dislocation, and the frontal cortex (defined as one third anterior part of the cerebral

278 cortex) and hippocampus were immediately dissected and removed. Brain tissues were
279 homogenized in homogenization buffer [320 mM sucrose and 5 mM EDTA, containing
280 complete protease inhibitor cocktail tablet (Complete Mini; Roche, Mannheim,
281 Germany)] and centrifuged at $1,000 \times g$ for 10 min. The supernatant was centrifuged at
282 $12,000 \times g$ for 10 min, and the resultant pellet was re-suspended in homogenization
283 buffer as the P2 fraction. The P2 fraction was layered over a 1.2 M/0.8 M sucrose
284 gradient and centrifuged at $90,000 \times g$ for 2 h. The synaptosome fraction was collected
285 from the interface, mixed with equal volume of Triton solution [1% Triton X-100, 0.32
286 M sucrose, 12 mM Tris-Cl (pH 8.0)] for 15 min, and centrifuged at $200,000 \times g$ for 1 h.
287 The resultant pellet was suspended in 40 mM Tris-Cl (pH 8.0), 1% SDS as the post
288 synaptic density (PSD) fraction. The protein concentration was determined using BCA
289 Protein Assay Reagent (Thermo Fisher Scientific, MA, USA). Equal volume of SDS
290 sample buffer [125 mM Tris-Cl (pH 6.8), 4% SDS, 20% glycerol, 0.002% BPB, 2%
291 2-mercaptoethanol] was added to the sample fractions and boiled for 5 min at 100 °C.

292 Protein samples were separated by 8% SDS-PAGE and electrophoretically
293 transferred to nitrocellulose membranes (GE Healthcare, NJ, USA). Both WT and
294 GluD1-KO mice samples were blotted on the same membrane for quantification.
295 Membranes were blocked with 5% skimmed milk in TBS-T [20 mM Tris-Cl (pH 7.6),
296 137 mM NaCl, 0.1% Tween 20] for 1 h, and incubated with each primary antibody (1
297 $\mu\text{g/ml}$) (Table 1) for 3-4 h and horseradish peroxidase-conjugated secondary antibody
298 for 1 h. Between these incubation steps, membranes were washed three times with
299 TBS-T for 30 min. Protein bands were visualized with an enhanced chemiluminescence
300 (ECL) kit (GE Healthcare) using a luminescence image analyzer with an electronically
301 cooled charge-coupled device camera (EZ capture MG; ATTO, Tokyo, Japan). Signal

302 intensities of immunoreacted bands were determined using CS Analyzer ver.3.0
303 (ATTO).

304

305 **Table 1.** Primary antibodies used in the present study

306

	Sequence (NCBI #)	RRID	Host	Specificity	Reference/Source
GluA1	841-907 aa (X57497)	AB_2571752	Rb	KO	FI (GluA1-Rb-Af690)
GluA1	880-907 aa	n/a	Rb	IB	[80]
GluA2	175-430 aa (NM_013540)	AB_2113875	Ms		Millipore (MAB397)
GluN2A	1126-1408 aa	AB_2571605	Rb	KO	[81] FI (GluRe1C-Rb-Af542)
GluN2B	1301-1456 aa (D10651)	AB_2571762	Rb	KO	FI(GluRe2C-Rb-Af300)
GluK2	844-908 aa (P42269)	n/a	Rb	KO	[82] Synaptic systems (180 003)
GluD1	895-932 aa (NM_008166)	AB_2571757	Rb	KO	[32] FI (GluD1C-Rb-Af1390)
GluD2	897-934 aa (D13266)	AB_2571601	Rb	KO	[68]
PSD-95	1-64 aa (D50621)	AB_2571611	Rb	IB	[83] FI (PSD-95-Rb-Af1720)

307

308 aa, amino acid residues; FI, Frontier Institute; GluA1, AMPA-type glutamate receptor-1;

309 GluA2, AMPA-type glutamate receptor-2; GluD1, delta-type glutamate receptor-1;

310 GluD2, delta-type glutamate receptor-2; GluK2, kainate-type glutamate receptor-2;

311 GluN2A, N-methyl-D-aspartate glutamate receptor-2A; GluN2B, N-methyl-D-aspartate

312 glutamate receptor-2B; GP, guinea pig polyclonal antibody; KO, lack of

313 immunohistochemical or immunoblot labeling in knockout mice; Ms, mouse monoclonal
314 antibody; Rb, rabbit polyclonal antibody; RRID, Research Resource Identifier.
315

316 **Statistical analysis**

317 All data are expressed as mean \pm SEM. Statistical analyses for behavioral studies were
318 performed using EZR (Saitama Medical Center, Jichi Medical University, Saitama,
319 Japan), which is a graphical user interface for R (The R Foundation for Statistical
320 Computing, Vienna, Austria). Data were analyzed by one-way ANOVA, two-way
321 ANOVA, two-way repeated-measures ANOVA followed by Dunnett's post hoc tests, or
322 Student's t-test with Welch's correction as appropriate to correct for multiple
323 comparisons. Attack latency in the resident-intruder test was analyzed using
324 Kaplan-Meier survival curves followed by Mantel-Cox log-rank tests. All statistical
325 tests were two-tailed. The level of significance set was $p < 0.05$.
326

327 **Results**

328 **Normal anxiety-related behavior in GluD1-KO mice**

329 To determine whether GluD1 was involved in anxiety-related behavior, we performed
330 tests in an open field (Fig 1A), an elevated plus maze (Fig 1F), and a light-dark transition
331 test (Fig 1M). It is well established that performance in both the open field and elevated
332 plus maze are influenced by the arena illumination levels [84,85]. We therefore used two
333 different illumination conditions (5 and 100 lux) in these tests.
334

335 **Fig 1. Hyperlocomotor activity but normal anxiety-related behavior in GluD1-KO**
336 **mice.** (A-E) The open field. Schematic representation of the open field test (A).
337 GluD1-KO mice traveled significantly longer than WT in the open field test with 5 lux
338 illumination (WT, n = 19; GluD1-KO, n = 13; $p < 0.05$, unpaired Student's *t*-test) (B), and
339 100 lux (WT, n = 33; GluD1-KO, n = 24; $p < 0.05$) (D). No significant difference was
340 observed in the time spent in the central region with 5 lux ($p = 0.46$) (C) or 100 lux ($p =$
341 0.08) illumination (E). (F-L) The elevated plus maze. Schematic representation of the
342 elevated plus maze (F). There were no significant differences between WT (5 lux, n = 16;
343 100 lux, n = 21) and GluD1-KO mice (5 lux, n = 10; 100 lux, n = 19) in the time spent in
344 the closed arms [5 lux, $p = 0.87$ (G); 100 lux, $p = 0.25$ (J)] or in the open arms [5 lux, $p =$
345 0.95 (H); 100 lux, $p = 0.72$ (K)], or in the number of entries into the open arms [5 lux, $p =$
346 0.92 (I); 100 lux, $p = 0.70$ (L)]. (M-P) The light-dark transition test. Schematic
347 representation of the light-dark transition test (M). There was no significant difference
348 between WT (n = 33) and GluD1-KO mice (n = 23) in the time spent in the dark and light
349 boxes [Dark box, $p = 0.62$; Light box, $p = 0.62$ (N)], in the number of entries into the light
350 box ($p = 0.85$) (O), or in latency to first transition into the light box ($p = 0.17$) (P). * $p <$
351 0.05 , unpaired Student's *t*-test with Welch's correction. All values presented are mean \pm
352 SEM.

353

354 We performed the open field test for a total duration of 10 min (Fig 1A). The open
355 field test presents a conflict between innate drives to explore a novel environment and
356 personal safety [86]. GluD1-KO mice traveled longer distances compared to WT mice
357 under both illumination conditions (Fig 1B, D). We also calculated the percentage of time
358 spent in the central area of the open field, which is commonly used as an index of anxiety

359 [41]. There were no significant differences in the percentage of time spent in the central
360 area between WT and GluD1-KO mice under either illumination conditions (Fig 1C, E).

361 In the elevated plus maze, we did not detect any significant differences in the time
362 spent in the closed or open arms between genotypes, or in the number of entries into the
363 open arm between genotypes under either of the illumination conditions (Fig 1G–L).
364 There was no significant differences between WT and GluD1-KO mice in total distance
365 traveled using 5 lux (WT, 15.6 ± 1.0 meters; GluD1-KO, 18.3 ± 0.96 meters; $p = 0.076$)
366 or 100 lux (WT, 19.5 ± 0.96 meters; GluD1-KO, 21.7 ± 1.1 meters; $p = 0.142$) and no
367 differences in total entries using 5 lux (WT, 26 ± 2.4 ; GluD1-KO, 30 ± 2.8 ; $p = 0.256$) or
368 100 lux (WT, 34 ± 2.0 ; GluD1-KO, 39 ± 2.4 ; $p = 0.162$).

369 Besides, we performed another behavioral assay for studying anxiety in mice, the
370 light-dark transition test (Fig 1M). There was no significant difference between WT and
371 GluD1-KO mice in the time spent in the light and dark portions of the box (Fig 1N), in
372 transition number between the illuminated and dark areas (Fig 1O), or in latency to enter
373 the illuminated area of the box (Fig 1P).

374 Together, GluD1-KO mice showed hyper-locomotor activity in the open field test;
375 however, GluD1-KO mice did not show any anxiety-related behaviors in the open field,
376 elevated plus maze, or light-dark transition tests.

377

378 **Normal aggression-like behavior in GluD1-KO mice**

379 GluD1-KO mice were rare to show aggressive-like behavior in their home cage. In
380 accordance with these observations, both latency to attack first and attack frequency in
381 GluD1-KO mice were not significantly different from that of WT mice in the
382 resident-intruder test (Fig 2).

383

384 **Fig 2. Normal aggression-like behavior in GluD1-KO mice.** In the resident-intruder
385 test, there was no significant difference between WT (n = 8) and GluD1-KO (n = 7)
386 mice in attack latency (left; log-rank test, $\chi^2 = 2.451$, p = 0.117) or attack frequency
387 (right, unpaired student's *t*-test, p = 0.304). All values presented are mean \pm SEM.

388

389 **Normal sensorimotor gating in GluD1-KO mice**

390 Because human mutations of the *Grid1* gene are associated with schizophrenia [23–25],
391 we next performed PPI of the acoustic startle response, which is one of the most
392 promising electrophysiological endophenotypes of both patients and animal models of
393 schizophrenia [87–90]. In the acoustic startle responses, the amplitude of startle
394 responses was dependent on pulse intensity. There was no difference between genotypes
395 (Fig 3A).

396 We then examined PPI levels of WT and GluD1-KO mice using four different
397 prepulse intensities. Induction of PPI using 73-, 76-, 79- and 82-dB prepulse in the
398 120-dB startle condition occurred in both WT and GluD1-KO mice (Fig 3B). There was
399 no significant difference between WT and GluD1-KO mice in PPI levels, suggesting
400 normal sensorimotor gating in GluD1-KO mice.

401

402 **Fig 3. Normal startle response and prepulse inhibition in GluD1-KO mice.** (A)

403 Acoustic startle reflex test: Startle responses amplitudes were dependent on pulse
404 intensity (WT, n = 7; GluD1-KO, n = 9) (two-way ANOVA: $F_{7,112} = 24.2$, p < 0.001).

405 There was no difference between genotype ($F_{1,112} = 0.08$, p = 0.78), and no interaction

406 between genotype and tone intensity ($F_{7,112} = 0.13$, p = 1.00). (B) Prepulse inhibition test:

407 The PPI levels of WT (n = 11) and GluD1-KO mice (n = 12) were not significantly
408 different with prepulses of 73, 76, 79 and 82 dB (two-way ANOVA: Genotype; $F_{1,84} =$
409 2.64, $p = 0.11$). PPI levels were dependent on prepulse intensity ($F_{3,84} = 18.09$, $p < 0.001$).
410 There was no significant interaction between genotype and prepulse intensity ($F_{3,84} = 0.08$,
411 $p = 0.97$). All values presented are mean \pm SEM.

412

413 **Social deficiency in GluD1-KO mice**

414 We then examined the three-chamber social interaction test, which consists of a
415 sociability test and a social novelty preference test [48] (Fig 4). In the sociability test, a
416 wire cage with a stranger mouse (Stranger 1) was placed in one of the side chambers, and
417 an empty cage was placed in another side chamber (Fig 4A). The preference of the mouse
418 can be quantified based on the time spent around the wire cage with a stranger mouse
419 versus the empty cage. GluD1-KO mice spent a significantly shorter time around the wire
420 cage with the stranger mouse than that of WT mice (Fig 4B) indicating a lack of
421 sociability.

422 In the social novelty preference test, a second stranger mouse (Stranger 2) was
423 introduced into the empty cage. GluD1-KO mice spent a significantly shorter time around
424 the wire cage with the novel stranger mouse (stranger 2) than that of WT mice (Fig 4C)
425 indicating a lack of preference for social novelty.

426

427 **Fig 4. Reduced sociability and preference for social novelty in GluD1-KO mice.** (A)

428 Schematic representation of the three-chamber social interaction test. Sociability test
429 (middle): a wire cage with a stranger mouse (Stranger 1) was placed in one side chamber
430 and an empty wire cage was placed on the opposite side chamber. Social novelty

431 preference test (right): a novel stranger mouse (Stranger 2) was placed in a wire cage in
432 one side chamber and a familiar mouse (Stranger 1) was placed in a wire cage on the
433 opposite site. (B) Sociability test: there was a significantly lower time spent near the wire
434 cage with Stranger 1 in GluD1-KO (n = 23) than that of WT mice (n = 25) ($p < 0.01$). (C)
435 Social novelty preference test: there was significantly lower time spent near the wire cage
436 with stranger 2 in GluD1-KO mice than that of WT mice ($p < 0.05$). All values presented
437 are mean \pm SEM. * $p < 0.05$; ** $p < 0.01$, unpaired Student's t-test with Welch's
438 correction.

439

440 **Impaired contextual fear memories in GluD1-KO mice**

441 To assess the involvement of GluD1 in fear memory, we performed contextual and cued
442 fear conditioning tests (Fig 5). The freezing responses in the conditioning session did not
443 differ significantly between genotypes (Fig 5A). In the contextual test, GluD1-KO mice
444 exhibited a modest but significant decrease in the freezing response relative to WT mice
445 (Fig 5B).

446 In contrast, GluD1-KO mice showed no significant difference in freezing response
447 relative to WT mice in the cued test (Fig 5C). There were no significant differences in
448 pain sensitivity (Fig 5D) or hearing ability (Fig 3A) between genotypes, suggesting that
449 ablation of GluD1 caused deficits of contextual, but not cued memories in the fear
450 conditioning tests.

451

452 **Fig 5. Impaired contextual, but not cued memory in GluD1-KO mice in the fear**

453 **conditioning test.** (A) Schematic representation of the conditioning test (left). Freezing
454 responses on the conditioning test; there was no significant difference between WT (n =

455 8) and GluD1-KO (n = 9) mice (two-way repeated-measures ANOVA: Genotype; $F_{1,15} =$
456 0.0075, $p = 0.93$, US presentation; $F_{3,45} = 14.5$, $p < 0.0001$, Genotype \times US presentation;
457 $F_{3,45} = 0.523$, $p = 0.67$). (B) Contextual test: freezing responses on the contextual testing
458 24 h after conditioning. There was significantly lower freezing in GluD1-KO mice during
459 contextual conditioning ($p < 0.01$, unpaired Student's t-test). (C) Cued test: freezing
460 responses on the cued testing 48 h after conditioning. There was no significant difference
461 between WT and GluD1-KO mice in cued conditioning during pre-tone and tone
462 (pre-tone, $p = 0.62$; tone, $p = 0.14$; unpaired Student's t-test). (D) Pain sensitivity test;
463 there were no significant differences between WT (n = 14) and GluD1-KO (n = 11)
464 mice in the footshock test evaluated by flinch ($p=0.24$), vocalization ($p=0.24$), vertical
465 jump ($p=0.91$) and horizontal jump ($p=0.56$). All values presented are mean \pm SEM. ** p
466 < 0.01 .

467

468 **Restoring depression-like behavior in GluD1-KO mice using a** 469 **serotonin transporter blocker**

470 To analyze depression-like behavior, we used the Porsolt forced-swim test [72] (Fig 6).
471 GluD1-KO mice showed significantly increased immobility, indicating enhanced
472 depressive-like behavior (Fig 6A).

473

474 **Fig 6. Enhanced depressive-like behavior in GluD1-KO mice.** (A) Schematic
475 representation of the forced-swim test (left). There was significantly higher percentage
476 immobility in GluD1-KO mice (n = 22) than WT (n = 30) (middle) (two-way repeated
477 measures ANOVA: Genotype, $F_{1,50} = 5.66$, $p < 0.05$; Time, $F_{4,200} = 25.1$, $p < 0.001$;

478 Genotype \times Time, $F_{4,200} = 1.56$, $p = 0.19$). Average immobility times for minutes 1 to 5 in
479 the forced-swim test (right). There was a significantly higher immobility in GluD1-KO
480 than WT mice ($p < 0.05$, unpaired Student's t-test). (B) Impact of antidepressants on the
481 forced-swim test. Animals were injected intraperitoneally with saline (WT, $n = 12$;
482 GluD1-KO, $n = 8$), imipramine (15 mg/kg) (WT, $n = 12$; GluD1-KO, $n = 8$), fluoxetine
483 (10 mg/kg) (WT, $n = 11$; GluD1-KO, $n = 9$), or desipramine (30 mg/kg) (WT, $n = 9$;
484 GluD1-KO, $n = 9$). Mice were subjected to open field test 60 min after injection for 10
485 min, and subsequently subjected to a forced-swim test for 5 min. Average immobility
486 times for 3 to 5 min: there was a significant genotype and treatment effect between and
487 WT and GluD1-KO mice (two-way ANOVA: Genotype, $F_{1,70} = 29.13$, $p < 0.001$; Drug,
488 $F_{3,70} = 6.16$, $p < 0.001$), but no significant interaction ($F_{3,70} = 2.56$, $p = 0.06$).
489 Within-genotype testing revealed that imipramine and fluoxetine led to a reduction in
490 immobility in GluD1-KO mice (one-way ANOVA with Dunnett's post hoc test: $F_{3,30} =$
491 5.58 , $p = 0.004$; Imipramine, $p = 0.0017$; Fluoxetine, $p = 0.032$; Desipramine, $p = 0.42$).
492 In WT mice, no significant differences in immobility were observed with these
493 antidepressants ($F_{3,40} = 1.78$, $p = 0.17$; Imipramine, $p = 0.85$, Fluoxetine, $p = 0.74$;
494 Desipramine, $p = 0.41$). All values presented are mean \pm SEM. * $p < 0.05$; ** $p < 0.01$,
495 Dunnett's post hoc test. Desi, desipramine; Flu, fluoxetine; Imi, imipramine.

496

497 Next, we tested the impact of representative antidepressants on depression-like
498 behavior in GluD1-KO mice. Imipramine and fluoxetine are inhibitors of the serotonin
499 transporter, while desipramine is an inhibitor of the norepinephrine transporter. [91,92].
500 These drugs were injected intraperitoneally into WT or GluD1-KO mice 70 min before
501 the forced-swim test (Fig 6B). Before the forced-swim test, an open field test (10 min)

502 was conducted to confirm that these drugs did not produce false-positive results on
503 restoring depression-like behavior in the forced-swim test due to an increase of locomotor
504 activity.

505 Injection of imipramine and desipramine, but not fluoxetine led to a reduction in
506 the total distance in WT mice (One-way ANOVA with Dunnett's post hoc test: $F_{3,40} =$
507 6.41 , $p = 0.0012$; Saline, 36.9 ± 2.3 meters; Imipramine, 25.5 ± 3.3 meters, $p = 0.035$;
508 Fluoxetine, 37.0 ± 1.4 meters, $p = 1.0$; Desipramine, 27.5 ± 1.9 meters, $p = 0.032$) in the
509 open field test). In contrast, no significant differences were observed in these
510 antidepressants in GluD1-KO mice ($F_{3,30} = 3.489$, $p = 0.028$; Saline, 37.6 ± 2.0 meters;
511 Imipramine, 31.7 ± 2.2 meters, $p = 0.10$; Fluoxetine, 38.1 ± 1.6 meters, $p = 1.0$;
512 Desipramine, 31.8 ± 1.8 meters, $p = 0.093$).

513 In the forced-swim test, no significant differences were observed in these
514 antidepressants in WT mice, possibly due to a ceiling effect. Of note, differences in
515 percentage immobility for the saline-injected versus naïve WT mice in the forced-swim
516 test may have arisen due to injection stress. Injected of GluD1-KO mice with imipramine
517 and fluoxetine, inhibitors of the serotonin transporter, led to a reduction in percentage
518 immobility in the forced-swim test (Fig 6B). In contrast, a reduction in percentage
519 immobility was not observed with GluD1-KO mice with desipramine, an inhibitor of the
520 norepinephrine transporter (Fig 6B). These results suggest that inhibition of the serotonin
521 transporter, but not norepinephrine transporter, restored depression-like behavior in
522 GluD1-KO mice.

523

524 **Normal glutamate receptor levels and expression of PSD-95**
525 **protein in the frontal cortex and hippocampus of GluD1-KO**
526 **mice**

527 Finally, we measured levels of synaptic protein expression in GluD1-KO mice. We
528 analyzed the excitatory synaptic proteins, such as AMPA
529 (α -amino-3-hydroxy-5-methyl-4-isoxazole propionic acid)-type (GluA1 and GluA2),
530 NMDA (N-methyl-D-aspartate)-type (GluN2A and GluN2B), Kainite-type (GluK2), and
531 δ -type (GluD2) glutamate receptors and PSD-95 in the synaptosome and PSD fractions
532 prepared from the frontal cortex and the hippocampus. Inconsistent with previous reports
533 [38,39], we did not observe significant alterations of protein expression levels in any of
534 these proteins in both synaptosome (Fig 7A) and PSD fractions (Fig 7B) in GluD1-KO
535 mice. What did, however, find small but significant increases in expression of GluD2 in
536 the PSD fractions of both the frontal cortex and the hippocampus of GluD1-KO mice (Fig
537 7B).

538

539 **Fig 7. Normal protein expression in synaptosome and PSD fractions prepared from**
540 **the frontal cortex and the hippocampus of GluD1-KO mice.** (A) Protein expression
541 in synaptosome fractions prepared from the frontal cortex and hippocampus. The
542 protein loaded in lanes for GluA1, GluA2, GluN2A, GluN2B, GluK2, and PSD-95 were
543 20 μ g, and 30 μ g for GluD2. There was no significant difference between WT and
544 GluD1-KO mice in the protein expression prepared from the synaptosome fractions of
545 the frontal cortex (GluA1, $p = 0.59$; GluA2, $p = 0.89$; GluN2A, $p = 0.34$; GluN2B, $p =$
546 0.33 ; GluK2, $p = 0.73$; GluD2, $p = 0.27$; PSD-95, $p = 0.71$) and the hippocampus

547 (GluA1, $p = 0.59$; GluA2, $p = 0.60$; GluN2A, $p = 0.96$; GluN2B, $p = 0.46$; GluK2, $p =$
548 0.86 ; GluD2, $p = 0.22$; PSD-95, $p = 0.50$). (B) Protein expression in PSD fractions
549 prepared from the frontal cortex and hippocampus. The protein loaded in lanes for
550 GluA1, GluA2, GluN2A, GluN2B, GluK2, and PSD-95 were $10 \mu\text{g}$, and $20 \mu\text{g}$ for
551 GluD2. Except for GluD2, there was no significant difference between WT and
552 GluD1-KO mice in protein expression prepared from the PSD fractions of the frontal
553 cortex (GluA1, $p = 0.50$; GluA2, $p = 0.99$; GluN2A, $p = 0.70$; GluN2B, $p = 0.43$;
554 GluK2, $p = 0.71$; GluD2, $p = 0.01$; PSD-95, $p = 0.68$) or the hippocampus (GluA1, $p =$
555 0.27 ; GluA2, $p = 0.76$; GluN2A, $p = 0.51$; GluN2B, $p = 0.49$; GluK2, $p = 0.50$; GluD2,
556 $p = 0.03$; PSD-95, $p = 0.89$). All values presented are mean \pm SEM from 3-4 experiments.
557 * $p < 0.05$, unpaired Student's t-test with Welch's correction. FC, the frontal cortex; HPC,
558 the hippocampus.

559

560 Discussion

561 To avoid the variability inherent in mixed genetic backgrounds and effects of closely
562 linked genes flanking the targeted locus, we generated GluD1-KO mice with a pure
563 C57BL/6N background and performed behavior analysis to assess GluD1 functions *in*
564 *vivo*. Our GluD1-KO mice showed hyperlocomotor activity, abnormal social behavior, a
565 deficit in contextual (but not cued) fear memory, and enhancement of depressive-like
566 behavior, that is partially consistent with the previous studies using *Grid1*^{tm1Jnz} mice
567 [37,38].

568 We did not observe significant differences in either aggressive behavior in the
569 resident-intruder test, anxiety-related behavior evaluated by the open field test or the
570 light-dark transition test, or the elevated plus maze in our GluD1-KO mice compared to
571 WT mice, whereas robust aggression and lower anxiety-related behavior were observed
572 in *Grid1*^{tm1Jnz} mice [37]. There are three conceivable possibilities that may explain the
573 different behavioral phenotypes between our GluD1-KO and the *Grid1*^{tm1Jnz} mice. The
574 first possibility is the strain difference and flanking-genes effect. It is known that there are
575 mouse-strain difference in basal levels of both aggression [44,45] and anxiety [41–43,93].
576 Moreover, it remains a concern that flanking alleles of the target locus generated during
577 the backcrossing of ES cell-derived knockout mice to appropriate mice strains may
578 influence phenotype [53,57,58]. The *Grid1*^{tm1Jnz} mouse was generated using the
579 129S6/SvEvTac ES cell line [40] followed by backcrossing to C57BL/6 strain 2–6 times
580 [37–39], so a phenotype difference may have arisen due to this. The second possibility is
581 deleterious effects of selection marker gene in the target locus on the neighboring genes
582 expression. The *Grid1*^{tm1Jnz} mouse harbors the neomycin phosphotransferase cassette
583 that allowed the selection of homologous recombinants in the targeted allele [40].
584 However, such marker genes can interfere with the transcription and splicing of the
585 neighboring genes, thereby resulting in ambiguous genotype-phenotype relationships
586 [64–67]. The gene encoding microRNA (miRNA) *miR-346* that regulates the translation
587 of mRNAs via interaction with their 3' untranslated regions, is located in intron 2 of the
588 GluD1 gene [94]. In contrast, the neomycin phosphotransferase cassette in our
589 GluD1-KO mice deleted via the Cre/loxP system, so it is more appropriate for analyses
590 of GluD1 function. The third possibility is a gene-environment interaction where

591 differences in laboratory environments becomes an additional contributing factor that
592 modulates the behavioral outcome of genetically modified animal models in psychiatry
593 [95,96].

594 We found that there was no significant alteration of postsynaptic protein
595 expression, including AMPA-, kainite-, and NMDA-type glutamate receptor subunits,
596 and PSD-95, in the frontal cortex or the hippocampus of GluD1-KO mice, which is
597 inconsistent with the previous studies [37–39]. In the prefrontal cortex, a significantly
598 lower expression of GluA1 and GluA2 was observed in *Grid1*^{tm1Jnz} mice [37]. In
599 addition, there was a significantly lower expression level of GluA1, GluA2, and GluK2,
600 and a significantly higher expression level of GluN2B and PSD-95 in the hippocampus of
601 *Grid1*^{tm1Jnz} mice [38]. In that study, the authors used a quantification method for
602 synaptosome fraction in which the optical density of each protein of interest was
603 normalized to β -actin [37,38]. In this case, however, normalization of synaptosome
604 fraction by β -actin might be an inappropriate method for two reasons. Firstly, β -actin is a
605 cytoplasmic protein and synaptosomal preparation may increase the variability of the
606 amount of β -actin proteins in the synaptosome fractions. Secondly, Gupta and colleagues
607 suggested that morphological abnormality in the hippocampus and the medial prefrontal
608 cortex in *Grid1*^{tm1Jnz} mice was probably due to an alteration of actin dynamics [39]. If
609 this was the case, then β -actin is not an appropriate protein for normalization. In contrast,

610 we investigated expression levels of synaptic proteins in synaptosome and PSD fractions
611 between WT and GluD1-KO mice using western blot without normalization by β -actin
612 (see Method). In addition, we confirmed that results of western blot for synaptosome and
613 PSD fractions without normalization were consistent with those on semi-quantitative
614 analysis using immunofluorescence [32,97–99].

615 In the fear conditioning test, GluD1-KO mice showed significantly lower freezing
616 times in contextual tests, but not in the cued tests. It is well known that the hippocampus
617 and amygdala are critical regions underlying contextual fear conditioning, whereas the
618 amygdala underlies cued conditioning [8]. The deficit of GluD1-KO mice in the
619 contextual test might suggest that GluD1 is more functionally important in the
620 hippocampus. Interestingly, forebrain-specific knockout mice of Cbln1, a partner
621 molecule of GluD1, showed a deficit in contextual and cued memory in the fear
622 conditioning test [100]. The GluD1-CBLN2-NRXN transsynaptic adhesion system
623 requires the formation and maintenance of synapses in the hippocampus *in vitro* and *ex*
624 *vivo* [1,2]. Moreover, Cbln1/2 double knockout mice have decreased synapse density in
625 the hippocampus of 6-month-olds but not 1- or 2-month-olds [3]. Of note, we observed
626 increased GluD2 expression in the PSD fraction of the hippocampus of GluD1-KO mice.
627 In contrast, increased GluD1 expression has been reported in the cerebellum of
628 GluD2-KO mice [9]. These results imply that compensatory regulation for GluD
629 subunits expression exists in brain regions, including the hippocampus. Further analysis
630 needs to clarify the specific role of the GluD-CBLN-NRXN transsynaptic adhesion
631 system in the hippocampus. In addition, there are reports that GluD1 also has unique
632 functions, such as (1) a regulator for group 5 mGluR-mediated AMPA-type glutamate

633 receptor trafficking [4], and (2) the ion channel activity via group 1 mGluR signaling
634 [5–7]. So, there are other possibilities that may explain how dysfunction of GluD1
635 affects hippocampal-dependent contextual fear memory. To determine details of the
636 molecular function of GluD1, the hippocampus is a suitable brain area for further
637 analyses.

638 Human GluD1 gene (*GRID1*) is a gene associated with susceptibility to
639 schizophrenia, autism spectrum disorder, and depression [23–28,94,101]. However,
640 how *GRID1* affects the pathophysiology of these conditions largely remains elusive.
641 Our GluD1-KO mice showed significantly lower sociability in the three-chambered
642 social interaction test, consistent with a previous report [37]. In contrast, our GluD1-KO
643 mice showed lower social novelty preference that is inconsistent with a previous report
644 [37]. Further analysis, such as novel object recognition, may clarify whether this
645 phenotype is derived from either impairment of memory function, sociability, or both.
646 Interestingly, lower *GRID1* mRNA expression is observed in the cerebral cortex of
647 patients with schizophrenia [94] and autism spectrum disorder [102]. Downregulation of
648 *GRID1* mRNA expression is also observed in iPS (induced pluripotent stem) cells
649 derived from Rett syndrome patients, which is a condition associated with autism
650 spectrum disorder [103]. In addition, downregulation of *Cbln1* mRNA was observed in
651 mice carrying a triple dose of *Ube3a*, a model mouse for autism spectrum disorder [104].
652 Deletion of *Cbln1* in the glutamatergic neurons of the ventral tegmental area led to
653 lower sociability by weakening excitatory synaptic transmission [104]. This behavioral
654 abnormality might support the hypothesis that GluD1-CBLN-NRXN-dependent synapse
655 formation and maintenance, in particular brain regions, is related to sociability.

656 Our GluD1-KO mice showed enhanced depressive-like behavior assessed by the
657 forced-swim test. Pharmacological studies further revealed that imipramine and
658 fluoxetine, but not desipramine, significantly restored the enhanced depressive-like
659 behavior in GluD1-KO mice. Because imipramine and fluoxetine are more effective in
660 inhibiting serotonin transporters than desipramine [91,92], increased serotonin
661 concentration in the brain regions related to depressive-like behavior may account for
662 the abnormal behavior of GluD1-KO mice; in other words, the serotonin signaling
663 pathway might be altered in GluD1-KO mice. Candidate regions, in which GluD1 is
664 expressed, related to depression are the lateral habenula and dorsal raphe nucleus
665 [32,33,100]. Increased neuronal activity in the lateral habenula is observed in patients
666 with depression and in animal models of depression [105,106] and lesions of the lateral
667 habenula alters extracellular serotonin concentration in the dorsal raphe nucleus when
668 receiving uncontrollable stress [107]. Furthermore, GluD1 mRNA is downregulated in
669 the frontal cortex of anhedonic rats as an animal model of depression [108], and this
670 phenotype is completely reversed by intraperitoneal injection of the antipsychotic
671 quetiapine [109]. Further analysis is required to identify regions involved in the
672 enhanced depressive-like behavior mediated by the serotonergic system in GluD1-KO
673 mice. As to the effect of antidepressants in the forced-swim test, selective serotonin
674 reuptake inhibitors (SSRIs) tend to lead to more swimming behavior, whereas serotonin
675 and norepinephrine reuptake inhibitors (SNRIs) tend to lead to more climbing behavior
676 [110,111]. Thus, evaluating climbing and swimming behavior with more specific SSRIs
677 (e.g. citalopram or escitalopram) [91,112] and SNRIs (e.g. reboxetine or atomoxetine)
678 [113] will allow us to more precisely discriminate the pathway underlying enhanced
679 depressive-like behavior in GluD1-KO mice.

680 Behavioral analyses under a pure C57BL/6N genetic background suggest that
681 GluD1 plays critical roles in contextual fear memory, sociability, and depressive-like
682 behavior. We originally developed the *Grid1*^{+/*flox*} mouse in which exon 4 of *Grid1* gene
683 was flanked by loxP sequences [68]. *Grid1*^{flox/*flox*} mice under a C57BL/6N genetic
684 background allow us to delete the *Grid1* gene in a brain region-specific manner using
685 region-specific Cre mice or Cre-expressing virus injections. This brain region-specific
686 GluD1-KO mouse could be a useful tool to clarify the neuronal circuits and molecular
687 mechanisms involved in contextual fear memory, sociability, and depressive-like
688 behavior.
689

690 **Acknowledgments**

691 We thank Akashi Kaori for technical assistance and advice; Moe Oono for drawing the
692 graphical illustrations; Hisaaki Namba, and Hiroyuki Nawa for the provision and help
693 with apparatus for the prepulse inhibition test; Hitoshi Uchida, Yu Ohmura, Shintaro
694 Ohtsuka, and Hidekazu Sotoyama for insightful comments and suggestions.
695

696 **Author contributions**

- 697 1. Conceptualization: CN, MA, KS.
- 698 2. Formal analysis: CN, TT.
- 699 3. Funding acquisition: TT, KS.

- 700 4. Investigation: CN.
701 5. Methodology: CN, MK, MA, KS.
702 6. Project administration: MA, KS.
703 7. Resources: EN, RN, MW.
704 8. Validation: CN, KT, TT.
705 9. Visualization: CN, TT.
706 10. Writing – original draft: CN, TT.
707 11. Writing – review & editing: CN, MK, KT, MW, MA, TT, KS.
708 All authors discussed the manuscript.
709

710 **Conflict of interest**

711 The authors declare no competing financial interests.
712

713 **Data Availability Statement**

714 All the raw data of behavioral tests (doi: 10.6084/m9.figshare.10052663) and western
715 blot images (doi: 10.6084/m9.figshare.10053092) in this study are disclosed in the
716 figshare.
717

718 **Funding**

719 This study was supported by Grants-in-Aid for Scientific Research (16H04650) and a
720 grant for Scientific Research on Innovative Areas (16H06276) from the Ministry of
721 Education, Culture, Sports, Science and Technology of Japan (MEXT) (to K.S.); Novo
722 Nordisk Foundation Young Investigator Award 2017 (NNF17OC0026774), Aarhus
723 Institute of Advanced Studies (AIAS)-EU FP7 Cofund programme (754513) and
724 Lundbeckfonden (DANDRITE-R248-2016-2518) (to T.T.).

725

726

727

728

729

730 **References**

- 731 1. Yamazaki M, Araki K, Shibata A, Mishina M. Molecular cloning of a cDNA
732 encoding a novel member of the mouse glutamate receptor channel family.
733 *Biochem Biophys Res Commun.* 1992;183: 886–892.
734 doi:10.1016/0006-291X(92)90566-4
- 735 2. Araki K, Meguro H, Kushiya E, Takayama C, Inoue Y, Mishina M. Selective
736 expression of the glutamate receptor channel delta 2 subunit in cerebellar Purkinje
737 cells. *Biochem Biophys Res Commun.* 1993;197: 1267–76.
738 doi:10.1006/bbrc.1993.2614
- 739 3. Lomeli H, Sprengel R, Laurie DJ, Köhr G, Herb A, Seeburg PH, et al. The rat
740 delta-1 and delta-2 subunits extend the excitatory amino acid receptor family.
741 *FEBS Lett.* 1993;315: 318–322. doi:10.1016/0014-5793(93)81186-4
- 742 4. Hirai H, Miyazaki T, Kakegawa W, Matsuda S, Mishina M, Watanabe M, et al.
743 Rescue of abnormal phenotypes of the delta2 glutamate receptor-null mice by
744 mutant delta2 transgenes. *EMBO Rep.* 2005;6: 90–5.
745 doi:10.1038/sj.embor.7400312

- 746 5. Kakegawa W, Kohda K, Yuzaki M. The delta2 “ionotropic” glutamate receptor
747 functions as a non-ionotropic receptor to control cerebellar synaptic plasticity. *J*
748 *Physiol.* 2007;584: 89–96. doi:10.1113/jphysiol.2007.141291
- 749 6. Kakegawa W, Miyazaki T, Hirai H, Motohashi J, Mishina M, Watanabe M, et al.
750 Ca²⁺ permeability of the channel pore is not essential for the delta2 glutamate
751 receptor to regulate synaptic plasticity and motor coordination. *J Physiol.*
752 2007;579: 729–35. doi:10.1113/jphysiol.2006.127100
- 753 7. Matsuda K, Miura E, Miyazaki T, Kakegawa W, Emi K, Narumi S, et al. Cbln1 is
754 a ligand for an orphan glutamate receptor delta2, a bidirectional synapse organizer.
755 *Science.* 2010;328: 363–8. doi:10.1126/science.1185152
- 756 8. Uemura T, Lee S-J, Yasumura M, Takeuchi T, Yoshida T, Ra M, et al.
757 Trans-synaptic interaction of GluRdelta2 and Neurexin through Cbln1 mediates
758 synapse formation in the cerebellum. *Cell.* 2010;141: 1068–79.
759 doi:10.1016/j.cell.2010.04.035
- 760 9. Tao W, Díaz-Alonso J, Sheng N, Nicoll RA. Postsynaptic δ 1 glutamate receptor
761 assembles and maintains hippocampal synapses via Cbln2 and neurexin. *Proc Natl*
762 *Acad Sci U S A.* 2018;115: E5373–E5381. doi:10.1073/pnas.1802737115

- 763 10. Ady V, Perroy J, Tricoire L, Piochon C, Dadak S, Chen X, et al. Type 1
764 metabotropic glutamate receptors (mGlu1) trigger the gating of GluD2 delta
765 glutamate receptors. *EMBO Rep.* 2014;15: 103–9. doi:10.1002/embr.201337371
- 766 11. Dadak S, Bouquier N, Goyet E, Fagni L, Levenes C, Perroy J. mGlu1 receptor
767 canonical signaling pathway contributes to the opening of the orphan GluD2
768 receptor. *Neuropharmacology.* 2017;115: 92–99.
769 doi:10.1016/J.NEUROPHARM.2016.06.001
- 770 12. Benamer N, Marti F, Lujan R, Hepp R, Aubier TG, Dupin AAM, et al. GluD1,
771 linked to schizophrenia, controls the burst firing of dopamine neurons. *Mol*
772 *Psychiatry.* 2018;23: 691–700. doi:10.1038/mp.2017.137
- 773 13. Takayama C, Nakagawa S, Watanabe M, Mishina M, Inoue Y. Light- and
774 electron-microscopic localization of the glutamate receptor channel 62 subunit in
775 the mouse Purkinje cell. *Neurosci Lett.* 1995;188: 89–92.
776 doi:10.1016/0304-3940(95)11403-J
- 777 14. Landsend AS, Amiry-Moghaddam M, Matsubara A, Bergersen L, Usami S,
778 Wenthold RJ, et al. Differential Localization of delta Glutamate Receptors in the
779 Rat Cerebellum: Coexpression with AMPA Receptors in Parallel Fiber-Spine

- 780 Synapses and Absence from Climbing Fiber-Spine Synapses. *J Neurosci.* 1997;17:
781 834–842. Available: <http://www.jneurosci.org/content/17/2/834.long>
- 782 15. Kashiwabuchi N, Ikeda K, Araki K, Hirano T, Shibuki K, Takayama C, et al.
783 Impairment of motor coordination, Purkinje cell synapse formation, and cerebellar
784 long-term depression in GluR δ 2 mutant mice. *Cell.* 1995;81: 245–252.
785 doi:10.1016/0092-8674(95)90334-8
- 786 16. Takeuchi T, Miyazaki T, Watanabe M, Mori H, Sakimura K, Mishina M. Control
787 of synaptic connection by glutamate receptor delta2 in the adult cerebellum. *J*
788 *Neurosci.* 2005;25: 2146–56. doi:10.1523/JNEUROSCI.4740-04.2005
- 789 17. Hirano T, Kasono K, Araki K, Shinozuka K, Mishina M. Involvement of the
790 glutamate receptor δ 2 subunit in the long-term depression of glutamate
791 responsiveness in cultured rat Purkinje cells. *Neurosci Lett.* 1994;182: 172–176.
792 doi:10.1016/0304-3940(94)90790-0
- 793 18. Kishimoto Y, Kawahara S, Suzuki M, Mori H, Mishina M, Kirino Y. Classical
794 eyeblink conditioning in glutamate receptor subunit δ 2 mutant mice is impaired in
795 the delay paradigm but not in the trace paradigm. *Eur J Neurosci.* 2001;13:
796 1249–1253. doi:10.1046/j.0953-816x.2001.01488.x

- 797 19. Katoh A, Yoshida T, Himeshima Y, Mishina M, Hirano T. Defective control and
798 adaptation of reflex eye movements in mutant mice deficient in either the
799 glutamate receptor $\delta 2$ subunit or Purkinje cells. *Eur J Neurosci*. 2005;21:
800 1315–1326. doi:10.1111/j.1460-9568.2005.03946.x
- 801 20. Kakegawa W, Miyazaki T, Emi K, Matsuda K, Kohda K, Motohashi J, et al.
802 Differential regulation of synaptic plasticity and cerebellar motor learning by the
803 C-terminal PDZ-binding motif of GluRdelta2. *J Neurosci*. 2008;28: 1460–8.
804 doi:10.1523/JNEUROSCI.2553-07.2008
- 805 21. Takeuchi T, Ohtsuki G, Yoshida T, Fukaya M, Wainai T, Yamashita M, et al.
806 Enhancement of Both Long-Term Depression Induction and Optokinetic Response
807 Adaptation in Mice Lacking Delphilin. Grant SGN, editor. *PLoS One*. 2008;3:
808 e2297. doi:10.1371/journal.pone.0002297
- 809 22. Kohda K, Kakegawa W, Matsuda S, Yamamoto T, Hirano H, Yuzaki M. The $\delta 2$
810 glutamate receptor gates long-term depression by coordinating interactions
811 between two AMPA receptor phosphorylation sites. *Proc Natl Acad Sci U S A*.
812 2013; 1218380110-. doi:10.1073/pnas.1218380110
- 813 23. Fallin MD, Lasseter VK, Avramopoulos D, Nicodemus KK, Wolyniec PS,
814 McGrath JA, et al. Bipolar I Disorder and Schizophrenia: A

- 815 440–Single-Nucleotide Polymorphism Screen of 64 Candidate Genes among
816 Ashkenazi Jewish Case-Parent Trios. *Am J Hum Genet.* 2005;77: 918–936.
817 doi:10.1086/497703
- 818 24. Guo S-Z, Huang K, Shi Y-Y, Tang W, Zhou J, Feng G-Y, et al. A case-control
819 association study between the GRID1 gene and schizophrenia in the Chinese
820 Northern Han population. *Schizophr Res.* 2007;93: 385–90.
821 doi:10.1016/j.schres.2007.03.007
- 822 25. Treutlein J, Mühleisen TW, Frank J, Mattheisen M, Herms S, Ludwig KU, et al.
823 Dissection of phenotype reveals possible association between schizophrenia and
824 Glutamate Receptor Delta 1 (GRID1) gene promoter. *Schizophr Res.* 2009;111:
825 123–130. doi:10.1016/j.schres.2009.03.011
- 826 26. Chen X, Lee G, Maher BS, Fanous AH, Chen J, Zhao Z, et al. GWA study data
827 mining and independent replication identify cardiomyopathy-associated 5
828 (CMYA5) as a risk gene for schizophrenia. *Mol Psychiatry.* 2011;16: 1117–29.
829 doi:10.1038/mp.2010.96
- 830 27. Muglia P, Tozzi F, Galwey NW, Francks C, Upmanyu R, Kong XQ, et al.
831 Genome-wide association study of recurrent major depressive disorder in two

- 832 European case-control cohorts. *Mol Psychiatry*. 2010;15: 589–601.
- 833 doi:10.1038/mp.2008.131
- 834 28. Glessner JT, Wang K, Cai G, Korvatska O, Kim CE, Wood S, et al. Autism
- 835 genome-wide copy number variation reveals ubiquitin and neuronal genes. *Nature*.
- 836 2009;459: 569–573. doi:10.1038/nature07953
- 837 29. Smith M, Spence MA, Flodman P. Nuclear and Mitochondrial Genome Defects in
- 838 Autisms. *Ann N Y Acad Sci*. 2009;1151: 102–132.
- 839 doi:10.1111/j.1749-6632.2008.03571.x
- 840 30. Griswold AJ, Ma D, Cukier HN, Nations LD, Schmidt MA, Chung R-H, et al.
- 841 Evaluation of copy number variations reveals novel candidate genes in autism
- 842 spectrum disorder-associated pathways. *Hum Mol Genet*. 2012;21: 3513–23.
- 843 doi:10.1093/hmg/dds164
- 844 31. Nord AS, Roeb W, Dickel DE, Walsh T, Kusenda M, O'Connor KL, et al.
- 845 Reduced transcript expression of genes affected by inherited and de novo CNVs in
- 846 autism. *Eur J Hum Genet*. 2011;19: 727–31. doi:10.1038/ejhg.2011.24
- 847 32. Konno K, Matsuda K, Nakamoto C, Uchigashima M, Miyazaki T, Yamasaki M, et
- 848 al. Enriched expression of GluD1 in higher brain regions and its involvement in

- 849 parallel fiber-interneuron synapse formation in the cerebellum. *J Neurosci.*
850 2014;34: 7412–24. doi:10.1523/JNEUROSCI.0628-14.2014
- 851 33. Hepp R, Hay YA, Aguado C, Lujan R, Dauphinot L, Potier MC, et al. Glutamate
852 receptors of the delta family are widely expressed in the adult brain. *Brain Struct*
853 *Funct.* 2015;220: 2797–2815. doi:10.1007/s00429-014-0827-4
- 854 34. Ryu K, Yokoyama M, Yamashita M, Hirano T. Induction of excitatory and
855 inhibitory presynaptic differentiation by GluD1. *Biochem Biophys Res Commun.*
856 2012;417: 157–61. doi:10.1016/j.bbrc.2011.11.075
- 857 35. Yasumura M, Yoshida T, Lee S, Uemura T, Joo J, Mishina M. Glutamate receptor
858 $\delta 1$ induces preferentially inhibitory presynaptic differentiation of cortical neurons
859 by interacting with neurexins through cerebellin precursor protein subtypes. *J*
860 *Neurochem.* 2012;121: 705–716. doi:10.1111/J.1471-4159.2011.07631.X
- 861 36. Suryavanshi PS, Gupta SC, Yadav R, Keshewani V, Liu J, Dravid SM. Glutamate
862 Delta-1 Receptor Regulates Metabotropic Glutamate Receptor 5 Signaling in the
863 Hippocampus. *Mol Pharmacol.* 2016;90: 96–105. doi:10.1124/mol.116.104786
- 864 37. Yadav R, Gupta SC, Hillman BG, Bhatt JM, Stairs DJ, Dravid SM. Deletion of
865 glutamate delta-1 receptor in mouse leads to aberrant emotional and social

- 866 behaviors. Christie B, editor. PLoS One. 2012;7: e32969.
867 doi:10.1371/journal.pone.0032969
- 868 38. Yadav R, Hillman BG, Gupta SC, Suryavanshi P, Bhatt JM, Pavuluri R, et al.
869 Deletion of Glutamate Delta-1 Receptor in Mouse Leads to Enhanced Working
870 Memory and Deficit in Fear Conditioning. Christie B, editor. PLoS One. 2013;8:
871 e60785. doi:10.1371/journal.pone.0060785
- 872 39. Gupta SC, Yadav R, Pavuluri R, Morley BJ, Stairs DJ, Dravid SM. Essential role
873 of GluD1 in dendritic spine development and GluN2B to GluN2A NMDAR
874 subunit switch in the cortex and hippocampus reveals ability of GluN2B inhibition
875 in correcting hyperconnectivity. Neuropharmacology. 2015;93: 274–284.
876 doi:10.1016/j.neuropharm.2015.02.013
- 877 40. Gao J, Maison SF, Wu X, Hirose K, Jones SM, Bayazitov I, et al. Orphan
878 glutamate receptor delta1 subunit required for high-frequency hearing. Mol Cell
879 Biol. 2007;27: 4500–12. doi:10.1128/MCB.02051-06
- 880 41. Crawley JN, Belknap JK, Collins A, Crabbe JC, Frankel W, Henderson N, et al.
881 Behavioral phenotypes of inbred mouse strains: implications and
882 recommendations for molecular studies. Psychopharmacology (Berl). 1997;132:
883 107–124. doi:10.1007/s002130050327

- 884 42. Holmes A, Li Q, Murphy DL, Gold E, Crawley JN. Abnormal anxiety-related
885 behavior in serotonin transporter null mutant mice: the influence of genetic
886 background. *Genes, Brain Behav.* 2003;2: 365–380.
887 doi:10.1046/j.1601-1848.2003.00050.x
- 888 43. Holmes A. Targeted gene mutation approaches to the study of anxiety-like
889 behavior in mice [Internet]. Pergamon; May 1, 2001 pp. 261–273.
890 doi:10.1016/S0149-7634(01)00012-4
- 891 44. Kessler S, Elliott GR, Orenberg EK, Barchas JD. A genetic analysis of aggressive
892 behavior in two strains of mice. *Behav Genet.* 1977;7: 313–21. Available:
893 <http://www.ncbi.nlm.nih.gov/pubmed/562156>
- 894 45. Mineur YS, Prasol DJ, Belzung C, Crusio WE. Agonistic Behavior and
895 Unpredictable Chronic Mild Stress in Mice. *Behav Genet.* 2003;33: 513–519.
896 doi:10.1023/A:1025770616068
- 897 46. Paylor R, Crawley JN. Inbred strain differences in prepulse inhibition of the mouse
898 startle response. *Psychopharmacology (Berl).* 1997;132: 169–80. Available:
899 <http://www.ncbi.nlm.nih.gov/pubmed/9266614>

- 900 47. Moy SS, Nadler JJ, Young NB, Perez A, Holloway LP, Barbaro RP, et al. Mouse
901 behavioral tasks relevant to autism: Phenotypes of 10 inbred strains. *Behav Brain*
902 *Res.* 2007;176: 4–20. doi:10.1016/J.BBR.2006.07.030
- 903 48. Moy SS, Nadler JJ, Perez A, Barbaro RP, Johns JM, Magnuson TR, et al.
904 Sociability and preference for social novelty in five inbred strains: an approach to
905 assess autistic-like behavior in mice. *Genes, Brain Behav.* 2004;3: 287–302.
906 doi:10.1111/j.1601-1848.2004.00076.x
- 907 49. Mogil JS, Wilson SG, Bon K, Eun Lee S, Chung K, Raber P, et al. Heritability of
908 nociception I: Responses of 11 inbred mouse strains on 12 measures of nociception.
909 *Pain.* 1999;80: 67–82. doi:10.1016/S0304-3959(98)00197-3
- 910 50. Mineur YS, Belzung C, Crusio WE. Effects of unpredictable chronic mild stress on
911 anxiety and depression-like behavior in mice. *Behav Brain Res.* 2006;175: 43–50.
912 doi:10.1016/J.BBR.2006.07.029
- 913 51. Lucki I, Dalvi A, Mayorga A. Sensitivity to the effects of pharmacologically
914 selective antidepressants in different strains of mice. *Psychopharmacology (Berl).*
915 2001;155: 315–322. doi:10.1007/s002130100694
- 916 52. Holmes A, Yang RJ, Murphy DL, Crawley JN. Evaluation of
917 antidepressant-related behavioral responses in mice lacking the serotonin

- 918 transporter. *Neuropsychopharmacology*. 2002;27: 914–23.
919 doi:10.1016/S0893-133X(02)00374-3
- 920 53. Gerlai R. Gene-targeting studies of mammalian behavior: is it the mutation or the
921 background genotype? *Trends Neurosci*. 1996;19: 177–181.
922 doi:10.1016/S0166-2236(96)20020-7
- 923 54. Wolfer DP, Müller U, Stagliar M, Lipp H-P. Assessing the effects of the 129/Sv
924 genetic background on swimming navigation learning in transgenic mutants: a
925 study using mice with a modified β -amyloid precursor protein gene. *Brain Res*.
926 1997;771: 1–13. doi:10.1016/S0006-8993(97)00673-2
- 927 55. Owen E., Logue S., Rasmussen D., J. M. Wehner. Assessment of learning by the
928 Morris water task and fear conditioning in inbred mouse strains and F1 hybrids:
929 implications of genetic background for single gene mutations and quantitative trait
930 loci analyses. *Neuroscience*. 1997;80: 1087–1099.
931 doi:10.1016/S0306-4522(97)00165-6
- 932 56. Balogh SA, Wehner JM. Inbred mouse strain differences in the establishment of
933 long-term fear memory. *Behav Brain Res*. 2003;140: 97–106.
934 doi:10.1016/S0166-4328(02)00279-6

- 935 57. Crusio WE. Flanking gene and genetic background problems in genetically
936 manipulated mice. *Biol Psychiatry*. 2004;56: 381–385.
937 doi:10.1016/J.BIOPSYCH.2003.12.026
- 938 58. Phillips TJ, Hen R, Crabbe JC. Complications associated with genetic background
939 effects in research using knockout mice. *Psychopharmacology (Berl)*. 1999;147:
940 5–7. doi:10.1007/s002130051128
- 941 59. Koike H, Arguello PA, Kvajo M, Karayiorgou M, Gogos JA. *Disc1* is mutated in
942 the 129S6/SvEv strain and modulates working memory in mice. *Proc Natl Acad
943 Sci U S A*. 2006;103: 3693–7. doi:10.1073/pnas.0511189103
- 944 60. Clapcote SJ, Roder JC. Deletion polymorphism of *Disc1* is common to all 129
945 mouse substrains: implications for gene-targeting studies of brain function.
946 *Genetics*. 2006;173: 2407–10. doi:10.1534/genetics.106.060749
- 947 61. Kuroda K, Yamada S, Tanaka M, Iizuka M, Yano H, Mori D, et al. Behavioral
948 alterations associated with targeted disruption of exons 2 and 3 of the *Disc1* gene
949 in the mouse. *Hum Mol Genet*. 2011;20: 4666–4683. doi:10.1093/hmg/ddr400
- 950 62. Blackwood DHR, Fordyce A, Walker MT, St. Clair DM, Porteous DJ, Muir WJ.
951 Schizophrenia and Affective Disorders—Cosegregation with a Translocation at
952 Chromosome 1q42 That Directly Disrupts Brain-Expressed Genes: Clinical and

- 953 P300 Findings in a Family. *Am J Hum Genet.* 2001;69: 428–433.
- 954 doi:10.1086/321969
- 955 63. Kilpinen H, Ylisaukko-oja T, Hennah W, Palo OM, Varilo T, Vanhala R, et al.
- 956 Association of DISC1 with autism and Asperger syndrome. *Mol Psychiatry.*
- 957 2008;13: 187–196. doi:10.1038/sj.mp.4002031
- 958 64. Fiering S, Epner E, Robinson K, Zhuang Y, Telling A, Hu M, et al. Targeted
- 959 deletion of 5'HS2 of the murine beta-globin LCR reveals that it is not essential for
- 960 proper regulation of the beta-globin locus. *Genes Dev.* 1995;9: 2203–13.
- 961 doi:10.1101/gad.9.18.2203
- 962 65. Mishina M, Sakimura K. Conditional gene targeting on the pure C57BL/6 genetic
- 963 background. *Neurosci Res.* 2007;58: 105–112.
- 964 doi:10.1016/J.NEURES.2007.01.004
- 965 66. Olson EN, Arnold HH, Rigby PWJ, Wold BJ. Know your neighbors: Three
- 966 phenotypes in null mutants of the myogenic bHLH gene MRF4 [Internet]. *Cell.*
- 967 Elsevier; 1996. pp. 1–4. doi:10.1016/S0092-8674(00)81073-9
- 968 67. Pham CT, MacIvor DM, Hug BA, Heusel JW, Ley TJ. Long-range disruption of
- 969 gene expression by a selectable marker cassette. *Proc Natl Acad Sci U S A.*
- 970 1996;93: 13090–5. doi:10.1073/PNAS.93.23.13090

- 971 68. Nakamoto C, Konno K, Miyazaki T, Nakatsukasa E, Natsume R, Abe M, et al.
972 Expression mapping, quantification, and complex formation of GluD1 and GluD2
973 glutamate receptors in adult mouse brain. *J Comp Neurol.* 2019;In press.
974 doi:10.1002/cne.24792
- 975 69. Nakamura K, Manabe T, Watanabe M, Mamiya T, Ichikawa R, Kiyama Y, et al.
976 Enhancement of hippocampal LTP, reference memory and sensorimotor gating in
977 mutant mice lacking a telencephalon-specific cell adhesion molecule. *Eur J*
978 *Neurosci.* 2001;13: 179–189. doi:10.1046/j.0953-816X.2000.01366.x
- 979 70. Katano T, Takao K, Abe M, Yamazaki M, Watanabe M, Miyakawa T, et al.
980 Distribution of Caskin1 protein and phenotypic characterization of its knockout
981 mice using a comprehensive behavioral test battery. *Mol Brain.* 2018;11: 63.
982 doi:10.1186/s13041-018-0407-2
- 983 71. Kato T, Kasai A, Mizuno M, Fengyi L, Shintani N, Maeda S, et al. Phenotypic
984 characterization of transgenic mice overexpressing neuregulin-1. *PLoS One.*
985 2010;5: e14185. doi:10.1371/journal.pone.0014185
- 986 72. Porsolt RD, Le Pichon M, Jalfre M. Depression: a new animal model sensitive to
987 antidepressant treatments. *Nature.* 1977;266: 730–732. doi:10.1038/266730a0

- 988 73. Redrobe JP, MacSweeney CP, Bourin M. The role of 5-HT1A and 5-HT1B
989 receptors in antidepressant drug actions in the mouse forced swimming test. *Eur J*
990 *Pharmacol.* 1996;318: 213–220. doi:10.1016/S0014-2999(96)00772-8
- 991 74. Vaugeois J-M, Passera G, Zuccaro F, Costentin J. Individual differences in
992 response to imipramine in the mouse tail suspension test. *Psychopharmacology*
993 (Berl). 1997;134: 387–391. doi:10.1007/s002130050475
- 994 75. Harkin AJ, Bruce KH, Craft B, Paul IA. Nitric oxide synthase inhibitors have
995 antidepressant-like properties in mice: 1. Acute treatments are active in the forced
996 swim test. *Eur J Pharmacol.* 1999;372: 207–213.
997 doi:10.1016/S0014-2999(99)00191-0
- 998 76. Wong EHF, Sonders MS, Amara SG, Tinholt PM, Piercey MFP, Hoffmann WP, et
999 al. Reboxetine: a pharmacologically potent, selective, and specific norepinephrine
1000 reuptake inhibitor. *Biol Psychiatry.* 2000;47: 818–829.
1001 doi:10.1016/S0006-3223(99)00291-7
- 1002 77. Zhang H, Li Z, Zhou Z, Yang H, Zhong Z, Lou C. Antidepressant-like effects of
1003 ginsenosides: A comparison of ginsenoside Rb3 and its four deglycosylated
1004 derivatives, Rg3, Rh2, compound K, and 20(S)-protopanaxadiol in mice models of

- 1005 despair. *Pharmacol Biochem Behav.* 2016;140: 17–26.
- 1006 doi:10.1016/J.PBB.2015.10.018
- 1007 78. Liu X, Gershenfeld HK. Genetic differences in the tail-suspension test and its
- 1008 relationship to imipramine response among 11 inbred strains of mice. *Biol*
- 1009 *Psychiatry.* 2001;49: 575–581. doi:10.1016/S0006-3223(00)01028-3
- 1010 79. Carlin RK. Isolation and characterization of postsynaptic densities from various
- 1011 brain regions: enrichment of different types of postsynaptic densities. *J Cell Biol.*
- 1012 1980;86: 831–845. doi:10.1083/jcb.86.3.831
- 1013 80. Yamazaki M, Fukaya M, Hashimoto K, Yamasaki M, Tsujita M, Itakura M, et al.
- 1014 TARPs gamma-2 and gamma-7 are essential for AMPA receptor expression in the
- 1015 cerebellum. *Eur J Neurosci.* 2010;31: 2204–20.
- 1016 doi:10.1111/j.1460-9568.2010.07254.x
- 1017 81. Watanabe M, Fukaya M, Sakimura K, Manabe T, Mishina M, Inoue Y. Selective
- 1018 scarcity of NMDA receptor channel subunits in the stratum lucidum (mossy
- 1019 fibre□recipient layer) of the mouse hippocampal CA3 subfield. *Eur J Neurosci.*
- 1020 1998;10: 478–487. doi:10.1046/j.1460-9568.1998.00063.x
- 1021 82. Watanabe-Iida I, Konno K, Akashi K, Abe M, Natsume R, Watanabe M, et al.
- 1022 Determination of kainate receptor subunit ratios in mouse brain using novel

- 1023 chimeric protein standards. *J Neurochem.* 2016;136: 295–305.
- 1024 doi:10.1111/jnc.13384
- 1025 83. Fukaya M, Watanabe M. Improved immunohistochemical detection of
- 1026 postsynaptically located PSD-95/SAP90 protein family by protease section
- 1027 pretreatment: A study in the adult mouse brain. *J Comp Neurol.* 2000;426:
- 1028 572–586. doi:10.1002/1096-9861(20001030)426:4<572::AID-CNE6>3.0.CO;2-9
- 1029 84. Valle FP. Effects of Strain, Sex, and Illumination on Open-Field Behavior of Rats.
- 1030 *Am J Psychol.* 1970;83: 103. doi:10.2307/1420860
- 1031 85. Griebel G, Moreau J-L, Jenck F, Martin JR, Misslin R. Some critical determinants
- 1032 of the behaviour of rats in the elevated plus-maze. *Behav Processes.* 1993;29:
- 1033 37–47. doi:10.1016/0376-6357(93)90026-N
- 1034 86. Crawley JN. Behavioral Phenotyping Strategies for Mutant Mice. *Neuron.*
- 1035 2008;57: 809–818. doi:10.1016/J.NEURON.2008.03.001
- 1036 87. Braff D, Stone C, Callaway E, Geyer M, Glick I, Bali L. Prestimulus Effects on
- 1037 Human Startle Reflex in Normals and Schizophrenics. *Psychophysiology.*
- 1038 1978;15: 339–343. doi:10.1111/j.1469-8986.1978.tb01390.x

- 1039 88. Grillon C, Ameli R, Charney DS, Krystal J, Braff D. Startle gating deficits occur
1040 across prepulse intensities in schizophrenic patients. *Biol Psychiatry*. 1992;32:
1041 939–43. Available: <http://www.ncbi.nlm.nih.gov/pubmed/1467378>
- 1042 89. Braff DL, Geyer MA. Sensorimotor Gating and Schizophrenia. *Arch Gen*
1043 *Psychiatry*. 1990;47: 181. doi:10.1001/archpsyc.1990.01810140081011
- 1044 90. Swerdlow NR, Braff DL, Taaid N, Geyer MA. Assessing the validity of an animal
1045 model of deficient sensorimotor gating in schizophrenic patients. *Arch Gen*
1046 *Psychiatry*. 1994;51: 139–54. Available:
1047 <http://www.ncbi.nlm.nih.gov/pubmed/8297213>
- 1048 91. Tatsumi M, Groshan K, Blakely RD, Richelson E. Pharmacological profile of
1049 antidepressants and related compounds at human monoamine transporters. *Eur J*
1050 *Pharmacol*. 1997;340: 249–258. doi:10.1016/S0014-2999(97)01393-9
- 1051 92. Owens MJ, Morgan WN, Plott SJ, Nemeroff CB. Neurotransmitter receptor and
1052 transporter binding profile of antidepressants and their metabolites. *J Pharmacol*
1053 *Exp Ther*. 1997;283: 1305–22. Available:
1054 <http://www.ncbi.nlm.nih.gov/pubmed/9400006>
- 1055 93. Crawley JN. Unusual behavioral phenotypes of inbred mouse strains. *Trends*
1056 *Neurosci*. 1996;19: 181–182. doi:10.1016/S0166-2236(96)20021-9

- 1057 94. Zhu Y, Kalbfleisch T, Brennan MD, Li Y. A MicroRNA gene is hosted in an intron
1058 of a schizophrenia-susceptibility gene. *Schizophrenia Research*. 2009.
1059 doi:10.1016/j.schres.2009.01.022
- 1060 95. Crabbe JC, Wahlsten D, Dudek BC. Genetics of Mouse Behavior: Interactions
1061 with Laboratory Environment. *Science* (80-). 1999;284. Available:
1062 <http://science.sciencemag.org/content/284/5420/1670.full>
- 1063 96. Razafsha M, Behforuzi H, Harati H, Wafai RA, Khaku A, Mondello S, et al. An
1064 updated overview of animal models in neuropsychiatry. *Neuroscience*. 2013;240:
1065 204–218. doi:10.1016/J.NEUROSCIENCE.2013.02.045
- 1066 97. Abe M, Fukaya M, Yagi T, Mishina M, Watanabe M, Sakimura K. NMDA
1067 receptor GluRepsilon/NR2 subunits are essential for postsynaptic localization and
1068 protein stability of GluRzeta1/NR1 subunit. *J Neurosci*. 2004;24: 7292–304.
1069 doi:10.1523/JNEUROSCI.1261-04.2004
- 1070 98. Akashi K, Kakizaki T, Kamiya H, Fukaya M, Yamasaki M, Abe M, et al. NMDA
1071 receptor GluN2B (GluR epsilon 2/NR2B) subunit is crucial for channel function,
1072 postsynaptic macromolecular organization, and actin cytoskeleton at hippocampal
1073 CA3 synapses. *J Neurosci*. 2009;29: 10869–82.
1074 doi:10.1523/JNEUROSCI.5531-08.2009

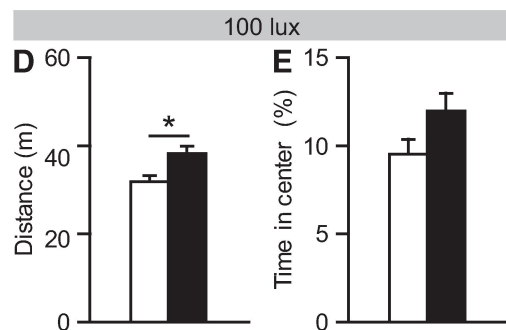
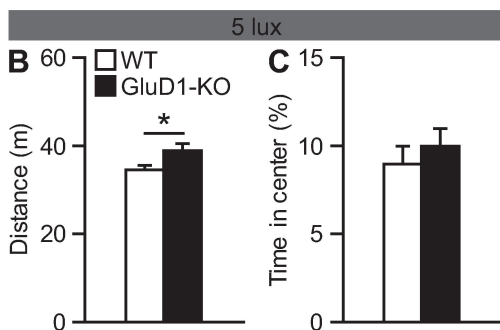
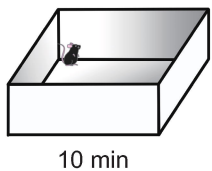
- 1075 99. Kawakami R, Shinohara Y, Kato Y, Sugiyama H, Shigemoto R, Ito I.
1076 Asymmetrical allocation of NMDA receptor epsilon2 subunits in hippocampal
1077 circuitry. *Science*. 2003;300: 990–4. doi:10.1126/science.1082609
- 1078 100. Otsuka S, Konno K, Abe M, Motohashi J, Kohda K, Sakimura K, et al. Roles of
1079 Cbln1 in Non-Motor Functions of Mice. *J Neurosci*. 2016;36: 11801–11816.
1080 doi:10.1523/JNEUROSCI.0322-16.2016
- 1081 101. Edwards AC, Aliev F, Bierut LJ, Bucholz KK, Edenberg H, Hesselbrock V, et al.
1082 Genome-wide association study of comorbid depressive syndrome and alcohol
1083 dependence. *Psychiatr Genet*. 2012;22: 31–41.
1084 doi:10.1097/YPG.0b013e32834acd07
- 1085 102. Garbett K, Ebert PJ, Mitchell A, Lintas C, Manzi B, Mirnics K, et al. Immune
1086 transcriptome alterations in the temporal cortex of subjects with autism. *Neurobiol*
1087 *Dis*. 2008;30: 303–311. Available:
1088 <https://www.sciencedirect.com/science/article/pii/S0969996108000247?via%3Di>
1089 [hub](#)
- 1090 103. Livide G, Patriarchi T, Amenduni M, Amabile S, Yasui D, Calcagno E, et al.
1091 GluD1 is a common altered player in neuronal differentiation from both

- 1092 MECP2-mutated and CDKL5-mutated iPS cells. *Eur J Hum Genet.* 2015;23:
1093 195–201. doi:10.1038/ejhg.2014.81
- 1094 104. Krishnan V, Stoppel DC, Nong Y, Johnson MA, Nadler MJS, Ozkaynak E, et al.
1095 Autism gene Ube3a and seizures impair sociability by repressing VTA Cbln1.
1096 *Nature.* 2017;543: 507–512. doi:10.1038/nature21678
- 1097 105. Li B, Piriz J, Mirrione M, Chung C, Proulx CD, Schulz D, et al. Synaptic
1098 potentiation onto habenula neurons in the learned helplessness model of
1099 depression. *Nature.* 2011;470: 535–539. doi:10.1038/nature09742
- 1100 106. Li K, Zhou T, Liao L, Yang Z, Wong C, Henn F, et al. CaMKII in Lateral
1101 Habenula Mediates Core Symptoms of Depression. *Science (80-).* 2013;341:
1102 1016–1020. doi:10.1126/science.1240729
- 1103 107. Amat J, Sparks PD, Matus-Amat P, Griggs J, Watkins LR, Maier SF. The role of
1104 the habenular complex in the elevation of dorsal raphe nucleus serotonin and the
1105 changes in the behavioral responses produced by uncontrollable stress. *Brain Res.*
1106 2001;917: 118–126. doi:10.1016/S0006-8993(01)02934-1
- 1107 108. Orsetti M, Di Brisco F, Canonico PL, Genazzani AA, Ghi P. Gene regulation in the
1108 frontal cortex of rats exposed to the chronic mild stress paradigm, an animal model

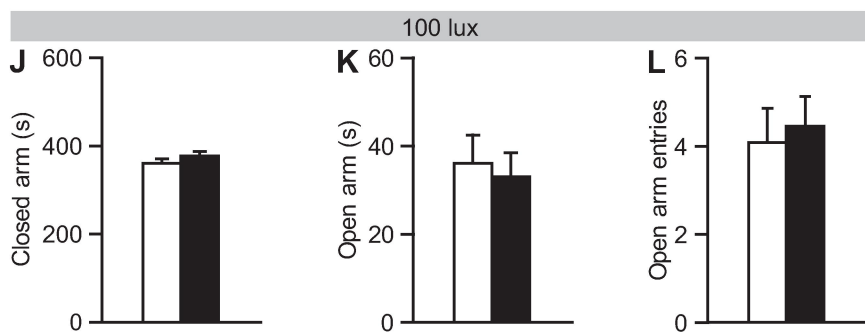
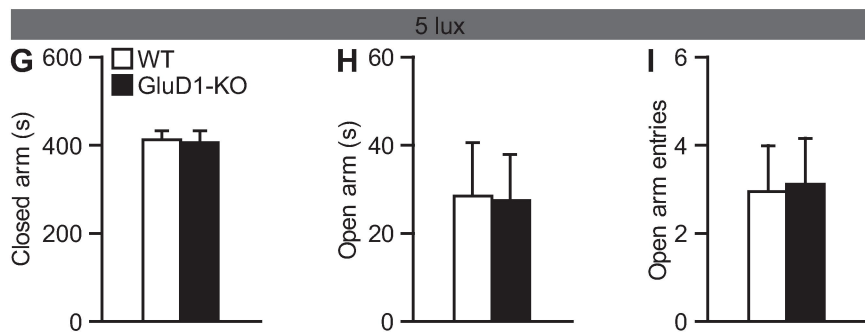
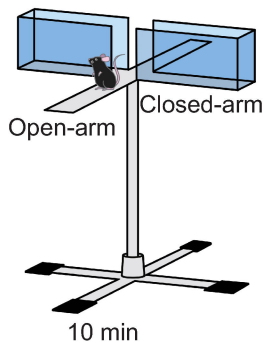
- 1109 of human depression. *Eur J Neurosci*. 2008;27: 2156–2164.
- 1110 doi:10.1111/j.1460-9568.2008.06155.x
- 1111 109. Orsetti M, Di Brisco F, Rinaldi M, Dallorto D, Ghi P. Some molecular effectors of
- 1112 antidepressant action of quetiapine revealed by DNA microarray in the frontal
- 1113 cortex of anhedonic rats. *Pharmacogenet Genomics*. 2009;19: 600–12.
- 1114 doi:10.1097/FPC.0b013e32832ee573
- 1115 110. Rénéric J-P, Lucki I. Antidepressant behavioral effects by dual inhibition of
- 1116 monoamine reuptake in the rat forced swimming test. *Psychopharmacology (Berl)*.
- 1117 1998;136: 190–197. doi:10.1007/s002130050555
- 1118 111. Detke MJ, Rickels M, Lucki I. Active behaviors in the rat forced swimming test
- 1119 differentially produced by serotonergic and noradrenergic antidepressants.
- 1120 *Psychopharmacology (Berl)*. 1995;121: 66–72. doi:10.1007/BF02245592
- 1121 112. Chen F, Larsen MB, Neubauer HA, Sanchez C, Plenge P, Wiborg O.
- 1122 Characterization of an allosteric citalopram-binding site at the serotonin
- 1123 transporter. *J Neurochem*. 2005;92: 21–28.
- 1124 doi:10.1111/j.1471-4159.2004.02835.x
- 1125 113. Bymaster F, Katner JS, Nelson DL, Hemrick-Luecke SK, Threlkeld PG,
- 1126 Heiligenstein JH, et al. Atomoxetine Increases Extracellular Levels of

- 1127 Norepinephrine and Dopamine in Prefrontal Cortex of Rat A Potential Mechanism
- 1128 for Efficacy in Attention Deficit/Hyperactivity Disorder.
- 1129 Neuropsychopharmacology. 2002;27: 699–711.
- 1130 doi:10.1016/S0893-133X(02)00346-9
- 1131

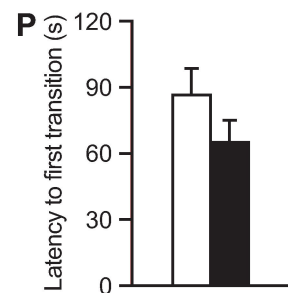
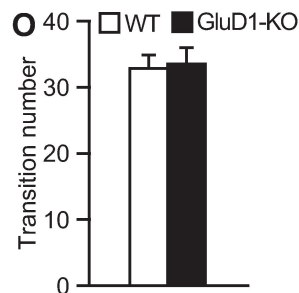
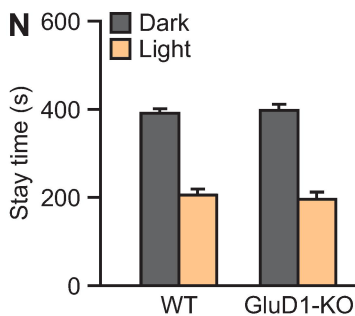
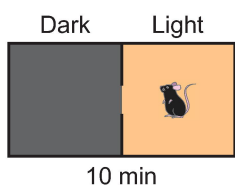
A Open-field test



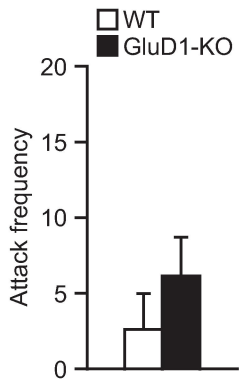
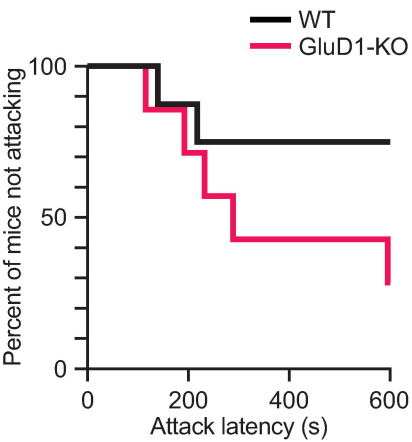
F Elevated plus maze test

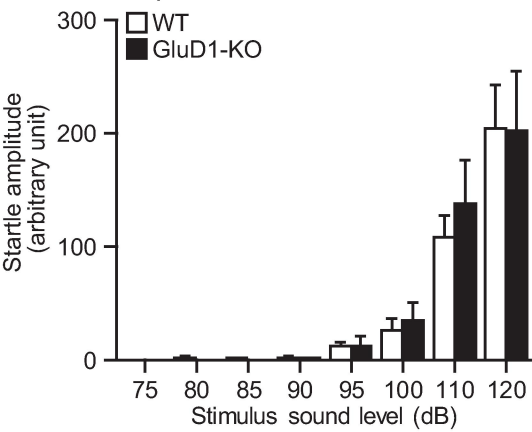
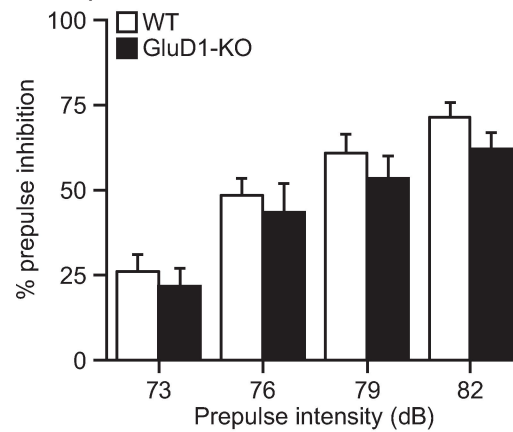


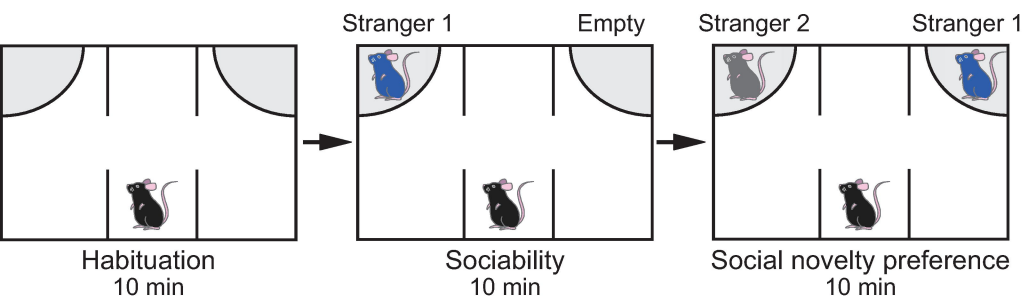
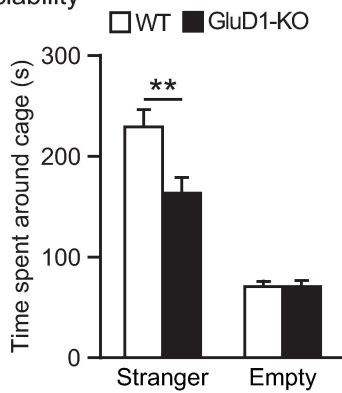
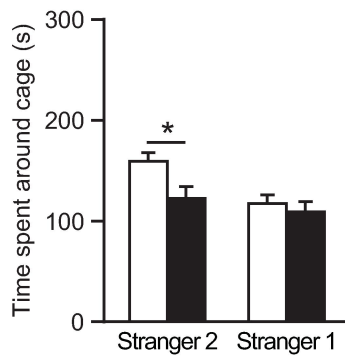
M Light-Dark transition test

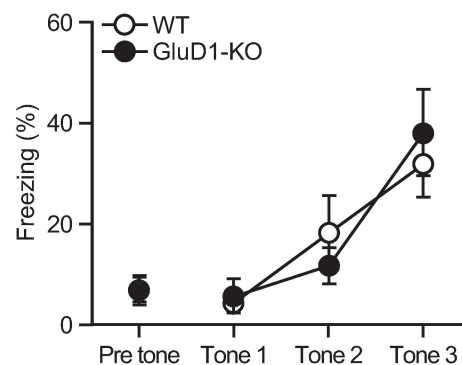
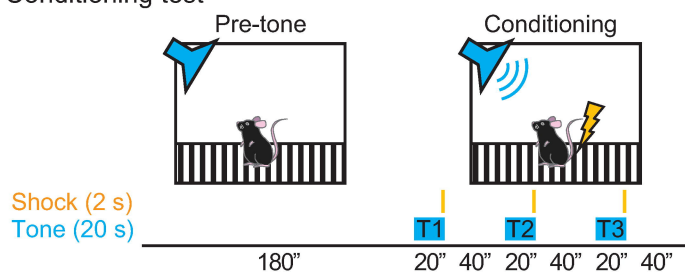
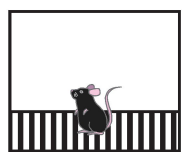


Resident-intruder test

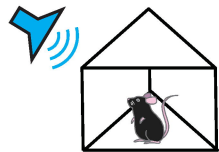


A Startle response**B** Prepulse inhibition

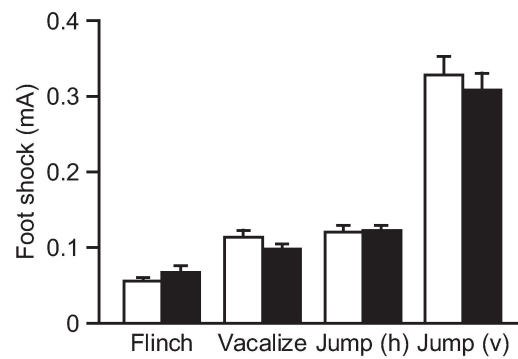
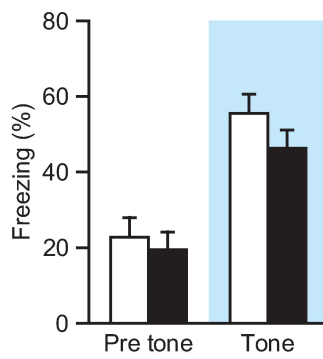
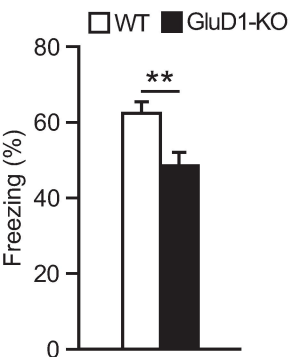
A Three-chambered social interaction test**B** Sociability**C** Social novelty preference

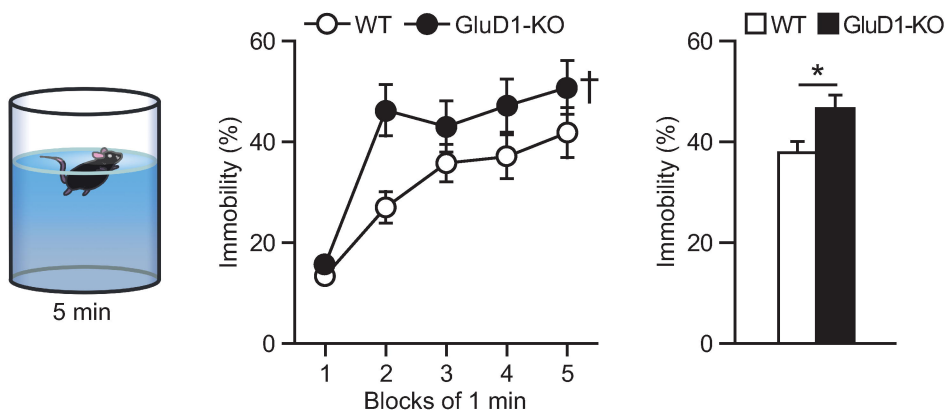
A Conditioning test**B Contextual test**

180"

C Cued test

Pre tone 60" Tone 180"

D Pain sensitivity

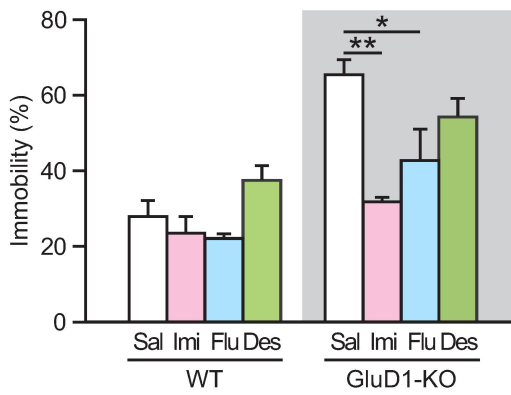
A Forced swim test**B** Forced swim test with pharmacology

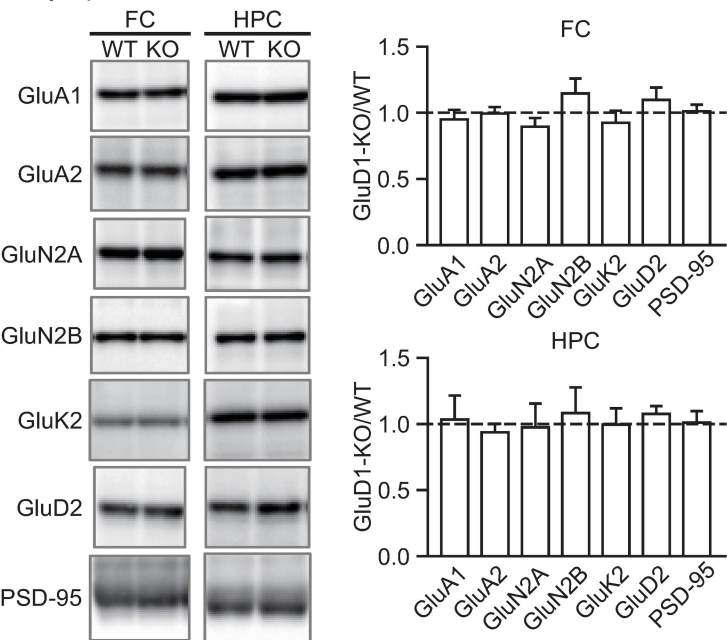
Drugs injection

60 min

Open-field test 10 min

5 min



A Synaptosome fraction**B** PSD fraction